# Propp's benzels and Lai's nearly symmetric hexagons with holes

Seok Hyun Byun<sup>a</sup> Mihai Ciucu<sup>b</sup> Yi-Lin Lee<sup>c</sup>

Submitted: Jan 14, 2025; Accepted: July 12, 2025; Published: Nov 3, 2025 © The authors. Released under the CC BY-ND license (International 4.0).

#### Abstract

In this paper we present a new version of the second author's factorization theorem for perfect matchings of symmetric graphs. We then use our result to solve four open problems of Propp on the enumeration of trimer tilings on the hexagonal lattice.

As another application, we obtain a semi-factorization result for the number of lozenge tilings of a large class of hexagonal regions with holes (obtained by starting with an arbitrary symmetric hexagon with holes, and translating all the holes one unit lattice segment in the same direction). This in turn leads to the solution of two open problems posed by Lai and to an extension of a result due to Fulmek and Krattenthaler, which results in exact enumeration formulas for some new families of hexagonal regions with holes.

Our result also allows us to find new, simpler proofs (and in one case, a new, simpler form) of some formulas due to Krattenthaler for the number of perfect matchings of Aztec rectangles with unit holes along a lattice diagonal.

Mathematics Subject Classifications: 05A15, 05A19

#### 1 Introduction

The second author's factorization theorem for perfect matchings of symmetric graphs [4, Theorem 1.2] opens up the possibility of simple proofs for results stating that the number of perfect matchings of a given family of symmetric planar graphs is expressed by an explicit product formula (see e.g. [1] [3] [5] [7] [8] [17] [25]).

Two particular classes of results of this kind concern honeycomb graphs with holes along a symmetry axis (for some illustrative examples, see [5]), and Aztec rectangles with holes along the axis of symmetry (see e.g. [4]). As it turns out, in both these cases

<sup>&</sup>lt;sup>a</sup>Department of Mathematics, Amherst College, Amherst, Massachusetts, USA (sbyun@amherst.edu).

 $<sup>^</sup>b$ Department of Mathematics, Indiana University, Bloomington, Indiana, USA (mciucu@iu.edu).

<sup>&</sup>lt;sup>c</sup>Department of Mathematics, National Taiwan Normal University, Taipei, Taiwan (yillee@ntnu.edu.tw).

interesting results hold also when the collection of holes is translated some distance away from the symmetry axis. Indeed, Krattenthaler proved such formulas for Aztec rectangles with unit holes (see [21]). Also, Lai conjectured (see [24]) that simple product formulas exist for the number of lozenge tilings of two families of regions, both obtained from symmetric hexagons with certain types of holes along the symmetry axis, by translating all the holes one unit lattice segment in the same direction<sup>1</sup>: one family corresponds to the holes being an arbitrary collection of like-oriented triangles of side-length two along the symmetry axis (the untranslated version of this is one of the families of regions for which a simple product formula is proved in [5]), while in the other there is a single hole in the shape of a shamrock, symmetric about the symmetry axis (the original, untranslated case is treated in [7] and [25], where a simple product formula is given for it). However, in both these situations the factorization theorem cannot be applied directly, because the dual graphs of the involved regions are not quite symmetric.

In this paper we present a new version (see Theorem 1) of [4, Theorem 1.2], which allows us to handle situations like the ones described above. In fact, it turns out that this leads to a quite general semi-factorization result<sup>2</sup> for the number of lozenge tilings of a large class of hexagonal regions with holes, obtained by starting with an arbitrary symmetric hexagon with holes, and then translating all the holes one unit lattice segment in the same direction (see Theorem 2).

In Section 3 we use Theorem 1 to solve four open problems of Propp (Problems 8 through 11 in [30]) on the enumeration of trimer tilings<sup>3</sup> on the hexagonal lattice.

Section 4 shows how Theorem 2 leads to the solution of the first open problems of Lai mentioned above. In Section 5 we discuss the second open problem of Lai (as well as some related problems), and then describe how to obtain explicit product formulas for the number of lozenge tilings of the regions appearing in those problems. In Section 6 we make further use of Theorem 2 to obtain an extension of a result due to Fulmek and Krattenthaler on the number of lozenge tilings of a symmetric hexagon containing a fixed lozenge just off the symmetry axis.

Theorem 1 also allows us to find new, simpler proofs (and in one case, a simpler form) of some formulas due to Krattenthaler for the number of perfect matchings of Aztec rectangles with unit holes along a lattice diagonal. We present this in Section 7.

# 2 Two general results

All the graphs in this section will be assumed to be bipartite. The two classes of vertices will be called white and black.

<sup>&</sup>lt;sup>1</sup>By identifying lozenge tilings of a region on the triangular lattice with perfect matchings of its planar dual, this is equivalent to enumerating perfect matchings of a honeycomb graph with holes.

<sup>&</sup>lt;sup>2</sup>As opposed to a factorization result, which expresses the quantity of interest as a product of two quantities of the same kind, pertaining to two "halves" of the original graph, a semi-factorization result expresses the quantity of interest as a *sum* of two such products.

<sup>&</sup>lt;sup>3</sup>More precisely, these are tilings by triples of contiguous unit hexagons, which in the dual picture become trimer coverings. For ease or reference we call them simply trimer tilings.

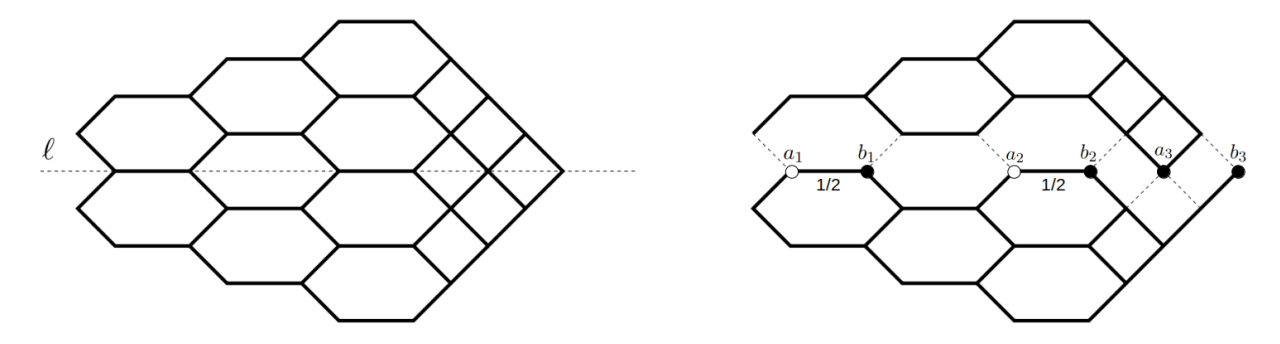


Figure 1: Illustrating Theorem 1(a): A plane bipartite symmetric graph G (left), and the resulting graphs  $G^+$  and  $G^-$  (right).

A perfect matching of a graph is a collection of vertex-disjoint edges that are collectively incident to all vertices. Given a graph G, we denote by M(G) the number of its perfect matchings. If v is a vertex of G, a v-near-perfect matching (or v-matching, for short) of G is a perfect matching of  $G \setminus v$ . We denote the number of v-matchings of G by  $M_v(G)$ . If v is not specified, we call a collection of disjoint edges of G that covers all but a single vertex of G a near-perfect matching.

Let G be a plane graph. We say that G is symmetric if it is invariant under the reflection across some straight line. The picture on the left in Figure 1 shows an example of a symmetric graph. Clearly, a symmetric graph has no perfect (resp., near-perfect) matching unless the axis of symmetry contains an even (resp., odd) number of vertices (otherwise, the total number of vertices of G has the wrong parity).

A weighted symmetric graph is a symmetric graph equipped with a weight function on the edges that is constant on the orbits of the reflection. The width of a symmetric graph G, denoted w(G), is defined to be the integer part of half the number of vertices of G lying on the symmetry axis.

Let G be a weighted symmetric graph with symmetry axis  $\ell$ , which we consider to be horizontal. Let  $a_1, b_1, a_2, b_2, \ldots$  be the vertices lying on  $\ell$ , as they occur from left to right (if G has an even number of vertices, this sequence ends with  $b_{w(G)}$ , while if G has an odd number of vertices, it ends with  $a_{w(G)+1}$ ).

The weight of a matching  $\mu$  is defined to be the product of the weights of the edges contained in  $\mu$ . The matching generating function of a weighted graph G, also denoted<sup>4</sup> by M(G), is the sum of the weights of all perfect matchings<sup>5</sup> of G. The matching generating function is clearly multiplicative with respect to disjoint unions of graphs. We will henceforth assume that all graphs under consideration are connected.

Let G be a weighted symmetric graph that is also bipartite. For definiteness, choose the leftmost vertex on the symmetry axis  $\ell$  to be white. We also assume that G has at least one vertex on the symmetry axis  $\ell$  (note that this implies that the symmetry is color-preserving; see the fifth paragraph of the proof of Theorem 1). We define two

 $<sup>^{4}</sup>$ When all weights are 1, this becomes just the number of perfect matchings of G.

<sup>&</sup>lt;sup>5</sup>For weighted graphs,  $M_v(G)$  denotes the sum of the weights of all v-near-perfect matchings of G.

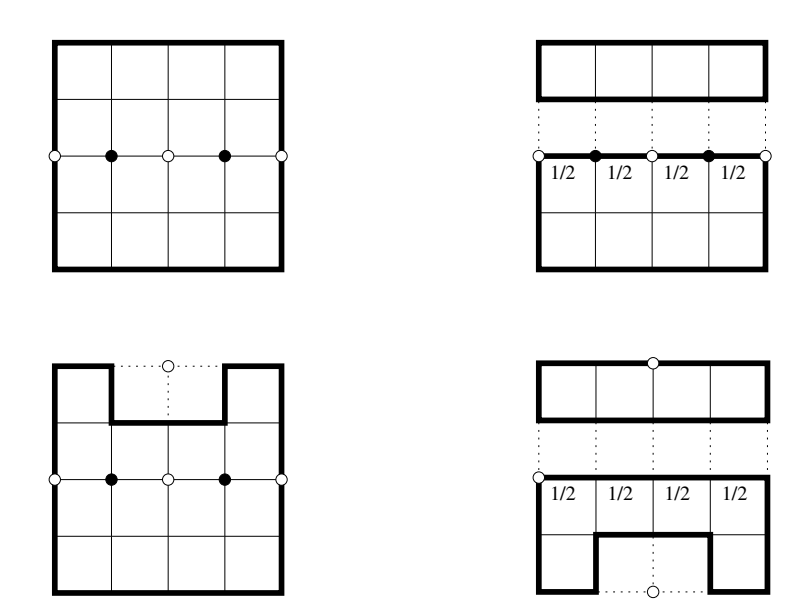


Figure 2: Illustrating the case of Theorem 1(b) when the removed boundary vertex v is white. A plane, bipartite symmetric graph G with an odd number of vertices on the symmetry axis, with the number of white vertices being one more than the number of black vertices (top left); the corresponding graphs  $G^+$  and  $G^-$  (top right). When a white vertex v is removed from the boundary (bottom left), the factorization involves the graphs  $G^+$  and  $G^- \setminus v'$ , where v' is the mirror image of v (bottom right).

subgraphs  $G^+$  and  $G^-$  as follows.

Given a vertex u of G on the symmetry axis, we call the operation of deleting all edges above  $\ell$  which are incident to u cutting above u; similarly, we call deleting all edges below  $\ell$  incident to u cutting below u. Perform cutting operations above all white  $a_i$ 's and black  $b_i$ 's and below all black  $a_i$ 's and white  $b_i$ 's. Note that this procedure yields cuts of the same kind at the endpoints of each edge lying on  $\ell$  (see the fourth paragraph in the proof of Theorem 1 for a justification). Reduce the weight of each such edge by half; leave all other weights unchanged.

As shown in the proof of Theorem 1(a), the graph  $G_0$  produced by the above procedure is disconnected into one part lying above and one lying below  $\ell$ . Denote the portion above  $\ell$  by  $G^+$ , and the one below  $\ell$  by  $G^-$ ; see the picture on the right in Figure 1 for an illustration of this procedure (the edges whose weight has been reduced by half are marked by 1/2).

Part (a) of the following result is a slight strengthening of the original factorization theorem of [4, Theorem 1.2] (namely, we show that the assumption made there that the graph is separated by its symmetry axis can be dropped). The new version is contained in part (b); its two cases are illustrated in Figures 2 and 3.

**Theorem 1.** Let G be a plane bipartite weighted symmetric graph. (a). If G has an even number of vertices, then

$$M(G) = 2^{w(G)} M(G^{+}) M(G^{-}).$$
 (1)

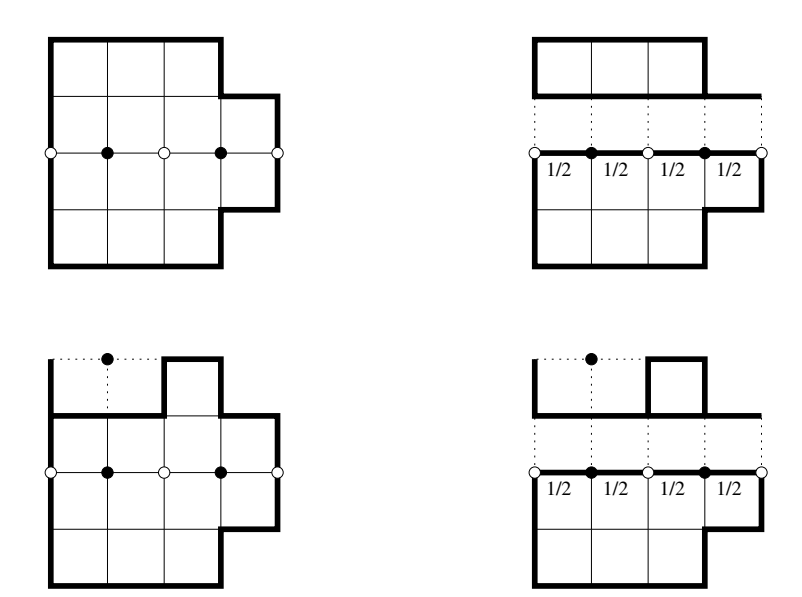


Figure 3: Illustrating the case of Theorem 1(b) when the removed boundary vertex v is black. A plane, bipartite symmetric graph G with an odd number of vertices on the symmetry axis, with one more black than white vertices (top left); the corresponding graphs  $G^+$  and  $G^-$  (top right). When a black vertex v is removed from the boundary (bottom left), the factorization involves the graphs  $G^+ \setminus v$  and  $G^-$  (bottom right).

(b). Suppose G has an odd number of vertices and v is a vertex on the unbounded face of G lying off the symmetry axis. Assume (without loss of generality, as G is symmetric) that v is above the symmetry axis. Then

$$M_{v}(G) = \begin{cases} 2^{w(G)} M(G^{+}) M_{v'}(G^{-}), & \text{if } v \text{ is white,} \\ 2^{w(G)} M_{v}(G^{+}) M(G^{-}), & \text{if } v \text{ is black,} \end{cases}$$
 (2)

where v' is the mirror image of v.

Proof. (a) This part is almost exactly the same as the second author's factorization theorem [4, Theorem 1.2]): the only difference is that one of the assumptions in the latter—namely, that the graph is separated by its symmetry axis (the meaning of this will be recalled below)—is not present in the statement of the current theorem. We show that this condition is in fact a consequence of the other assumptions (a fact overlooked at the time of writing of [4]). Then part (a) will follow directly from [4, Theorem 1.2].

The needed separation condition is that the graph  $G_0$  produced by the cutting procedure described before the statement of the theorem is disconnected into one part lying above and one lying below  $\ell$ . We show below that this is a consequence of the current assumptions.

What we need to show is that there exists a Jordan arc J in the plane connecting some point A on  $\ell$  to some point B on  $\ell$ —where A is to the left of  $a_1$ , and B is to the right of  $b_{\mathbf{w}(G)}$ —so that the portion H of  $G_0$  which is above or on  $\ell$  is above J, while the portion K of  $G_0$  which is below or on  $\ell$  is below J.

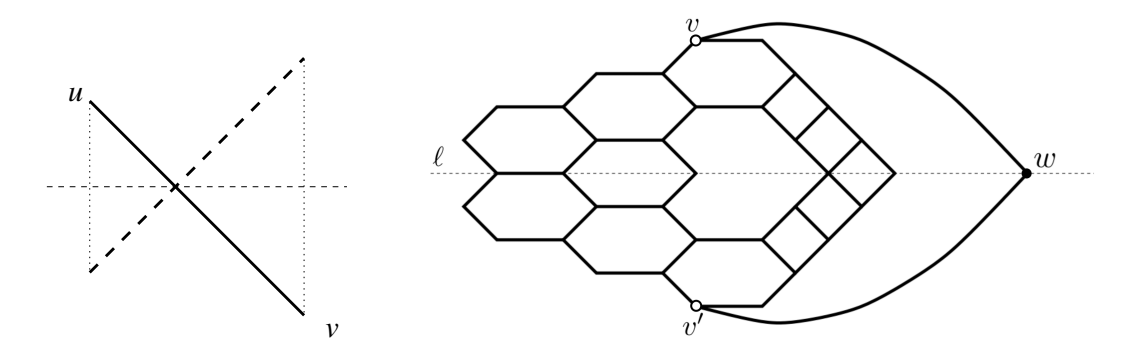


Figure 4: Left. Illustrating the argument in the fifth paragraph of the proof of Theorem 1. Right. The graph  $\overline{G}$  corresponding to the graph G shown in Figure 1 with one vertex removed (since the graph in Figure 1 has the same number of white and black vertices, we have to delete from it a vertex on  $\ell$  of the color opposite to the color of v in order to obtain a graph meeting the hypotheses of part (b) of Theorem 1).

To see this, note first that, as mentioned above, the cuts at the endpoints of each edge lying on  $\ell$  are of the same kind — both above, or both below  $\ell$ ; this is because we cut above white  $a_i$ 's and black  $b_i$ 's (and below black  $a_i$ 's and white  $b_i$ 's), and if an edge lies along  $\ell$ , its endpoints have on the one hand opposite color, and on the other opposite  $a_i$ -or  $b_i$ -type.

Secondly, note that  $G_0$  cannot have any edge  $\{u, v\}$  with u above  $\ell$  and v below  $\ell$ . Indeed, if u and v are not mirror images with respect to  $\ell$ , the symmetry of G implies that the mirror images u' and v' of u and v form another edge  $\{u', v'\}$  of  $G_0$ ; but then the edges  $\{u, v\}$  and  $\{u', v'\}$  would cross, which is a contradiction, since G is a plane graph (see the picture on the left in Figure 4). On the other hand, if u and v are mirror images of each other, let P be a path in G connecting u to  $a_1$  (as G is assumed to be connected, such a path exists). Then the mirror image P' of P across  $\ell$  is a path in G connecting v to  $a_1$ . Since P and P' have the same length and G is bipartite, it follows that u and v have the same color, so the edge  $\{u, v\}$  has endpoints of the same color; this contradicts the fact that G is bipartite.

The connected components of  $G_0 \cap \ell$  are either single vertices or paths with at least one edge. By the definition of  $G_0$ , all edges incident to a single-vertex component are confined to one side of  $\ell$ . Furthermore, by the second to last paragraph, all edges of  $G_0$  incident to the vertices of a path-component are also contained in one of the two half-planes bounding  $\ell$ . Therefore we can connect A to B by a Jordan arc J that stays close to  $\ell$  and meanders between the connected components of  $G_0 \cap \ell$  so that it does not cross any edge of  $G_0$  incident to a vertex on  $\ell$ . In fact, this arc J does not cross any other edge of  $G_0$  either. Indeed, as J can stay arbitrarily close to  $\ell$ , such an edge of  $G_0$  would need to have its endpoints on opposite sides of  $\ell$ , which we showed in the previous paragraph that is impossible. This proves our claim, and completes the proof of part (a).

(b) To prove the second part, note first that unless the difference between the number

of white and black vertices of G is  $\pm 1$ , and in addition v has the color of the majority of vertices, equation (2) holds trivially, as both sides equal zero. Therefore, without loss of generality we may assume that these conditions hold.

Next, define  $\overline{G}$  to be the graph obtained from G by including a new vertex w on  $\ell$  contained in the unbounded face of G, and the two new edges  $\{w,v\}$  and  $\{w,v'\}$  (both weighted by 1), where v' is the mirror image of v (see the picture on the right in Figure 4). Then  $\overline{G}$  is a plane, bipartite, weighted symmetric graph, to which part (a) of the theorem can be applied.

If v is white, it follows that w is black, and (since w is also a  $b_i$ -type vertex) the cutting operation at w prescribed by the factorization theorem occurs above w. Therefore,  $\overline{G}^+$  is precisely  $G^+$ . Furthermore, in  $\overline{G}^-$  vertex w has degree one, and after removing the edge  $\{u, v'\}$  that is forced to match it in every perfect matching, the resulting graph (which has the same matching generating function as  $\overline{G}^-$ , as the removed edge has weight 1) is precisely  $G^- \setminus v'$ . Thus part (a) of the theorem applied to  $\overline{G}$  yields

$$M(\overline{G}) = 2^{w(G)+1} M(G^+) M(G^- \setminus v') = 2^{w(G)+1} M(G^+) M_{v'}(G^-).$$
 (3)

On the other hand, since in  $\overline{G}$  the vertex w can only be matched to v or v', and since  $G \setminus v$  and  $G \setminus v'$  are isomorphic, it follows that  $M(\overline{G}) = 2 M(G \setminus v) = 2 M_v(G)$ . Combined with (3), this proves (2) when v is white. The case when v is black follows by the same argument.

The second result in this section is more specific, but is general enough to have several interesting consequences, including solutions to two open problems posed by Lai (see Sections 4 and 5), closed formulas for the number of lozenge tilings of some new families of hexagonal regions with holes (see Section 5), and an extension of a result by Fulmek and Krattenthaler (see Section 6).

Draw the triangular lattice so that one family of lattice lines is horizontal, and let H be a non-degenerate (i.e., with all sides of positive length) hexagonal region on this lattice, symmetric about a vertical symmetry  $\operatorname{axis}^6 \ell$ . Let  $R_0$  be the region obtained from H by removing an arbitrary collection  $\mathcal{C}$  of unit triangles, so that  $\mathcal{C}$  is symmetric about  $\ell$  and contains no unit triangles touching the southern or southeastern edge of H. Define R to be the region obtained from  $R_0$  by translating all unit triangles in  $\mathcal{C}$  one unit in the southeastern lattice direction. We call the region R a nearly symmetric hexagon with holes (an example is shown in the picture on the left in Figure 5). Therefore, while the outer, hexagonal boundary of the region R is symmetric with respect to the original symmetry axis  $\ell$ , the holes in R are symmetric about the line  $\ell'$ , the translation of  $\ell$  half a unit to the right.

Let G be the planar dual graph of R. Even though G is not symmetric about  $\ell'$ , let us consider the graphs  $G^+$  and  $G^-$  obtained from it by rotating it 90 degrees counterclockwise and performing cutting operations around the vertices on  $\ell'$  as prescribed by the

 $<sup>^6</sup>$ We will be interested in symmetric (or nearly-symmetric) regions obtained from H by making in it some holes, and since the symmetry of such regions seems to be more readily appreciated visually when the symmetry axis is vertical, we adopt this point of view for the second result in this section.

factorization theorem (assuming, in particular, that after the rotation the leftmost vertex on  $\ell'$  is white). In addition to these two graphs, consider also the graphs  $\widehat{G}^+$  and  $\widehat{G}^-$  obtained from G by performing cutting operations around the vertices on  $\ell'$  as prescribed by the factorization theorem, but assuming this time that after the rotation the leftmost vertex on  $\ell'$  is black. Define  $R^+$ ,  $R^-$ ,  $\widehat{R}^+$  and  $\widehat{R}^-$  to be the lattice regions whose planar duals are the graphs  $G^+$ ,  $G^-$ ,  $\widehat{G}^+$  and  $\widehat{G}^-$ , respectively<sup>7</sup>.

We can now state our second result in this section.

**Theorem 2.** Let R be a nearly symmetric hexagon with holes, and assume that the symmetric region  $R_0$  from which R was constructed admits at least one lozenge tiling. Then the number of lozenge tilings of R is given by

$$M(R) = 2^{w_{\ell'}(R)-1} \left( M(R^+) M(R^-) + M(\widehat{R}^+) M(\widehat{R}^-) \right),$$
 (4)

where  $w_{\ell'}(R)$  is half the number of unit triangles in R crossed by  $\ell'$ .

Remark 1. Formula (4) has the following amusing interpretation. The nearly symmetric hexagon with holes R is not quite symmetric about  $\ell'$ , but its holes are, so we might expect that if we form the expression on the right hand side of the factorization theorem (see equation (1)), the resulting number will be a reasonable estimate for M(R). But note: there are two ways to form this expression, depending on whether we consider the vertex  $a_1$  in the factorization theorem to be white or black! (For symmetric graphs, these two ways are equivalent, because they result in isomorphic pairs of graphs, due to the symmetry.) Form then both these expressions, and average them, to get an even more reasonable estimate. Then Theorem 2 states that this latter "estimate" is actually the exact value of M(R).

This phenomenon turns out to be very sensitive to changing the shape of the outer boundary of the region. For it to hold, it seems essential that the outer boundary is a symmetric hexagon, with symmetry axis half a unit away from the symmetry axis of the holes.

Our proof of the above theorem employs Kuo's graphical condensation [22]. Let G be a plane bipartite graph,  $V_1$  and  $V_2$  the vertex sets of the graph consisting of the two color classes, and E the edge set of the graph. For any subset  $W \subset V_1 \cup V_2$  of vertices of G, let  $G \setminus W$  be the subgraph obtained from G by deleting all vertices in W and all their incident edges.

<sup>&</sup>lt;sup>7</sup>If R is the region on the triangular lattice whose planar dual is the graph G, and G has weights on its edges, the lozenge position in R corresponding to any given edge of G comes weighted with the weight of that edge.

 $<sup>^{8}</sup>$ I.e. the region obtained from R by translating all the holes one unit lattice segment in the northwest direction.

<sup>&</sup>lt;sup>9</sup>We denote the matching generating function of the lozenge tilings of a region R (in which lozenge positions may carry weights) by M(R), because these lozenge tilings can be identified with perfect matchings of the (weighted) planar dual graph of the region R.

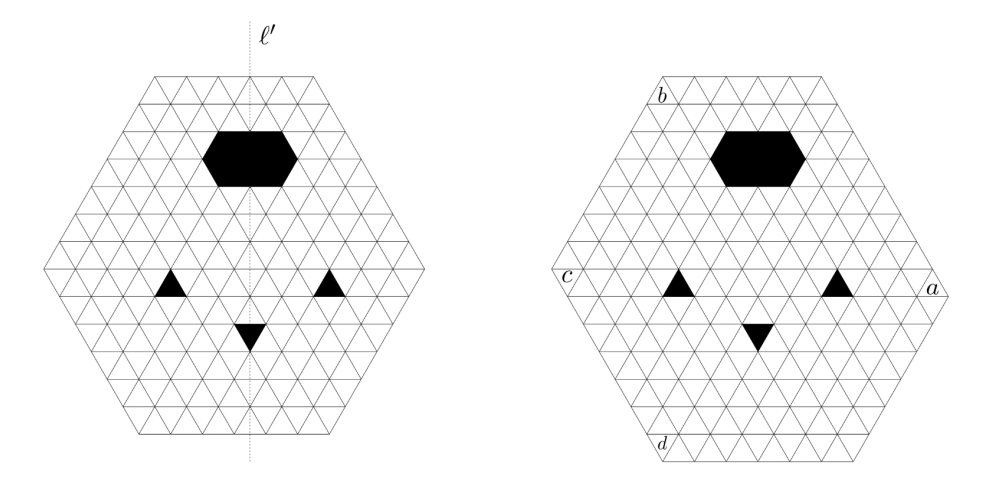


Figure 5: A nearly symmetric hexagon with holes R (left), and the extended region  $\widehat{R}$  (right). The positions of four unit triangles a, b, c, and d are marked on  $\widehat{R}$ .

**Theorem 3** (Theorem 5.2 in [22]). Let  $G = (V_1, V_2, E)$  be a weighted plane bipartite graph in which  $|V_1| = |V_2|$ . Let vertices a, b, c, and d appear in a cyclic order on the same face of G. If  $a, b \in V_1$  and  $c, d \in V_2$ , then

$$\mathcal{M}(G \setminus \{a,d\}) \, \mathcal{M}(G \setminus \{b,c\}) = \mathcal{M}(G) \, \mathcal{M}(G \setminus \{a,b,c,d\}) + \mathcal{M}(G \setminus \{a,c\}) \, \mathcal{M}(G \setminus \{b,d\}).$$

*Proof of Theorem* 2. The details are slightly different depending on the parity of the length of the top and the bottom side of the region R (there are  $2 \times 2 = 4$  cases). We present here the detailed arguments for the case when the top side is odd and the bottom side even; the other cases follow similarly.

We first add one layer of unit triangles on the bottom and bottom right side of R, as illustrated in Figure 5; denote the resulting region by  $\hat{R}$ , and call it the extended region. Choose the unit triangles a, b, c and d along the boundary of  $\hat{R}$  as indicated in the picture on the right in Figure 5 (the assumption that the outer boundary of R is a non-degenerate hexagon guarantees that a, b, c and d can be chosen as indicated). The dual graph of  $\hat{R}$  and the four vertices of it that correspond to a, b, c, and d satisfy the conditions in Kuo's graphical condensation theorem. Applying the latter and taking the duals of the resulting graphs, one gets the following recurrence relation (the six regions appearing in the recurrence are illustrated in Figure 6):

$$M(\hat{R} \setminus \{a, d\}) M(\hat{R} \setminus \{b, c\}) = M(\hat{R}) M(\hat{R} \setminus \{a, b, c, d\}) + M(\hat{R} \setminus \{a, c\}) M(\hat{R} \setminus \{b, d\}).$$
 (5)

Note that after removing some forced lozenges,  $\hat{R} \setminus \{a, d\}$  is precisely the region R whose tilings we want to enumerate (this is in fact what guided our construction of the extended region  $\hat{R}$ ), and  $\hat{R} \setminus \{b, c\}$  is a symmetric region (see the bottom left picture in Figure 6). Furthermore, each of the two regions  $\hat{R} \setminus \{a, b, c, d\}$  and  $\hat{R} \setminus \{a, c\}$  can be viewed as being obtained from a symmetric region with a unit dent on the boundary, by removing some forced lozenges (see the bottom center picture and top right picture, respectively, in

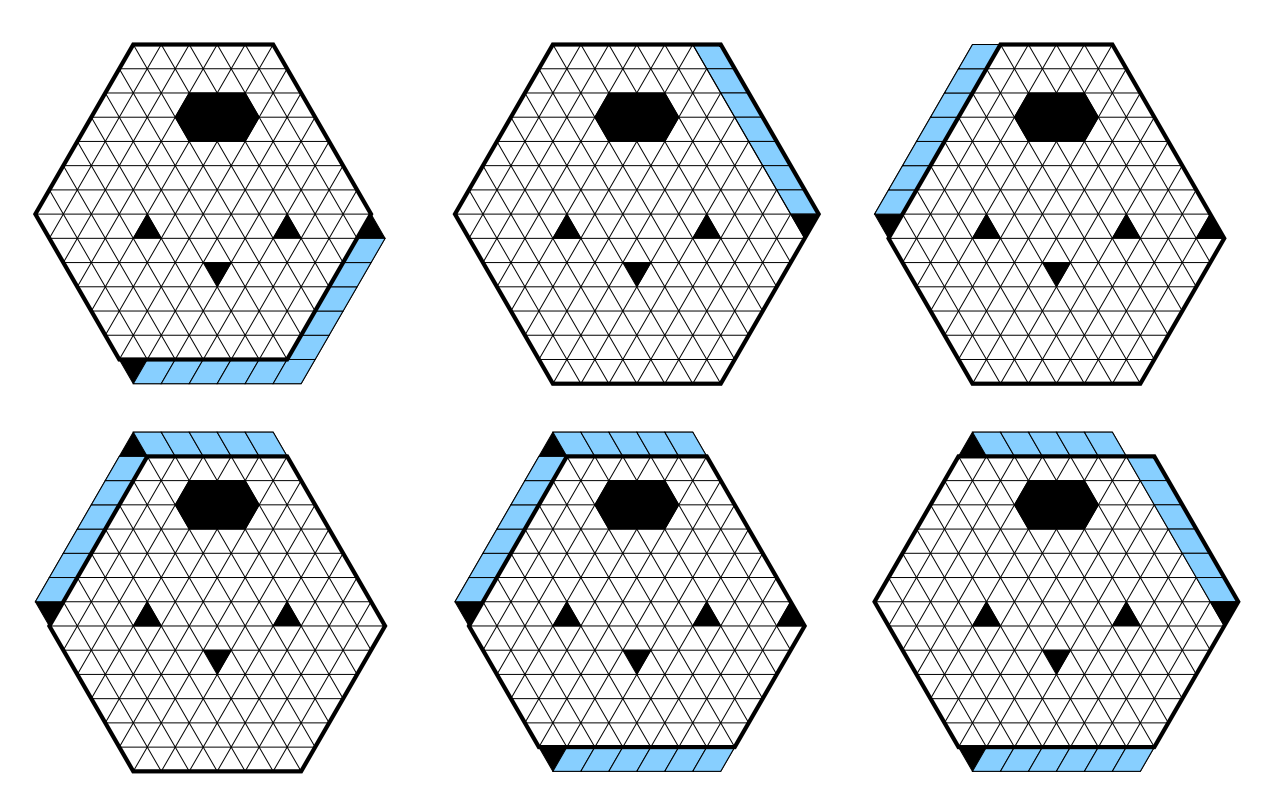


Figure 6: The six regions appearing in the recurrence obtained by applying Kuo condensation to the extended region  $\hat{R}$ , with the indicated choice of the unit triangles a,b,c, and d.

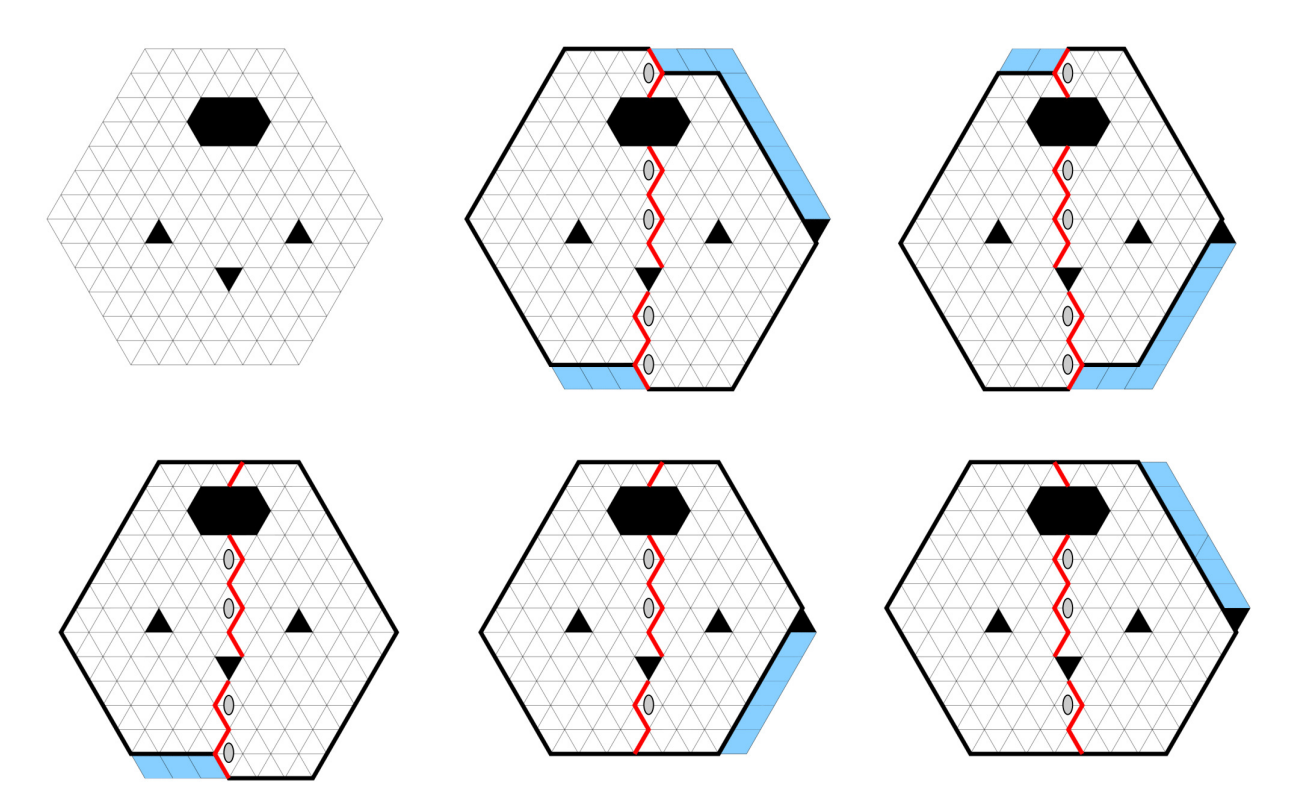


Figure 7: Applying Theorem 2.1 (a) and (b) to the five regions.

Figure 6). The remaining two regions  $\hat{R}$  and  $\hat{R} \setminus \{b,d\}$  are also equivalent to symmetric regions with a unit defect on the boundary, but we first need to enlarge them to see this. In the case of  $\hat{R}$ , we add one layer of unit triangles on the top right side of  $\hat{R}$ , and remove the bottom-most of these (see the top center picture in Figure 6). The region  $\hat{R} \setminus \{b,d\}$  can be handled similarly, but we first remove from it the forced lozenges along the top and bottom sides (see the bottom right picture in Figure 6).

Therefore, viewing the regions in (5) as described above, we can apply Theorem 1(a) to  $\hat{R}\setminus\{b,c\}$ , and Theorem 1(b) to the four regions  $\hat{R}$ ,  $\hat{R}\setminus\{a,b,c,d\}$ ,  $\hat{R}\setminus\{a,c\}$ , and  $\hat{R}\setminus\{b,d\}$ . When applying 10 Theorem 1, the powers of two in the factorizations of  $M(\hat{R}\setminus\{b,c\})$ ,  $M(\hat{R})$ , and  $M(\hat{R}\setminus\{a,c\})$  are  $2^{w_{l'}(R)}$ , while those in the factorizations of  $M(\hat{R}\setminus\{a,b,c,d\})$  and  $M(\hat{R}\setminus\{b,d\})$  are  $2^{w_{l'}(R)-1}$ . Figure 7 shows how the five regions are split via Theorem 1 (the shaded ellipses indicate lozenge positions weighted by 1/2); note that the first branch of Theorem 1(b) is applied when the unit boundary dent (which corresponds to v) has the same orientation as the top unit triangle along the symmetry axis (which corresponds to  $a_1$ ), and the second branch when the orientations are opposite. One readily sees that the resulting "half"-subregions — we call them parts — have the following properties:

(i) The left part of  $\hat{R} \setminus \{b,c\}$  is the same (up to forced lozenges) as the left part of

<sup>&</sup>lt;sup>10</sup>Strictly speaking, we apply Theorem 1 to their planar dual graphs, and then consider the regions whose planar duals are the resulting graphs.

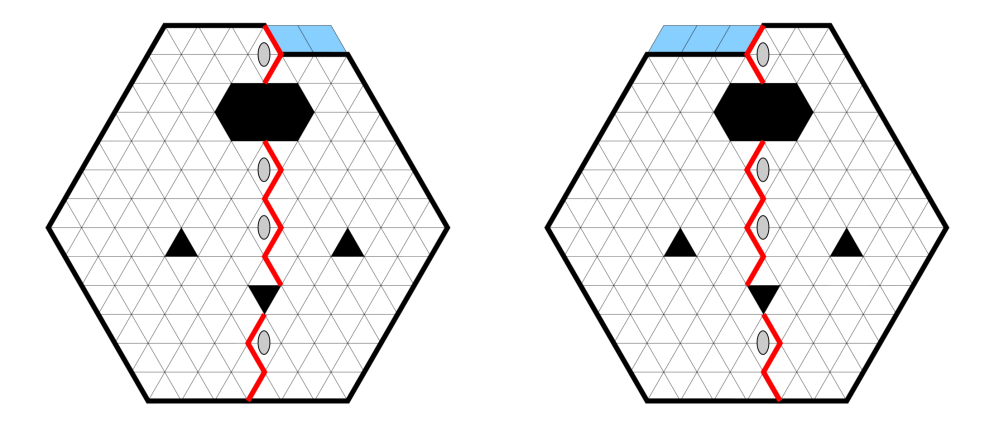


Figure 8: The two different ways of decomposing R into parts, using zigzag lines along  $\ell'$  as prescribed by the factorization theorem.

 $\hat{R} \setminus \{a, b, c, d\}$ , and the right part of  $\hat{R} \setminus \{b, c\}$  is the same (up to some forced lozenges) as the right part of  $\hat{R}$ .

- (ii) The left part of  $\hat{R} \setminus \{b, c\}$  is the same as the right part of  $\hat{R} \setminus \{b, d\}$ , and the right part of  $\hat{R} \setminus \{b, c\}$  is the same (up to forced lozenges) as the left part of  $\hat{R} \setminus \{a, c\}$ .
- (iii) The remaining two parts of  $\hat{R}$  and  $\hat{R} \setminus \{a, b, c, d\}$  (the ones which are not the same as any of the parts of  $\hat{R} \setminus \{b, c\}$ ) can be identified with the two parts of R obtained when we split R using one of the two zigzag lines along  $\ell'$ , as prescribed by the factorization theorem (compare the two picture at the center in Figure 7 and the left picture in Figure 8).
- (iv) The remaining two parts of  $\hat{R} \setminus \{a, c\}$  and  $\hat{R} \setminus \{b, d\}$  (the ones which cannot be identified with any part of  $\hat{R} \setminus \{b, c\}$ ), can be identified (up to forced lozenges) with the two parts of R when we split R using the other zigzag line along  $\ell'$ , as prescribed by the factorization theorem (compare the two pictures on the right in Figure 7 and the right picture in Figure 8).

By applying Theorem 1 to each of the five regions in (5) besides  $R \setminus \{a, d\}$  (which, as we pointed out, after removing the forced lozenges becomes precisely the region R whose tilings we want to enumerate), equation (5) becomes an equality in which the left hand side is the product of three factors, while the right hand side is the sum of two products, each having four factors.

By observations (i) and (ii) above, both factors on the left hand side besides  $M(\hat{R} \setminus \{a,d\})$  also appear in each of the two terms on the right hand side. By assumption,  $\hat{R} \setminus \{b,c\}$  (which is the same as the region  $R_0$ ) is tileable; hence, by Theorem 1, both these factors are non-zero. Dividing by them, the left hand side of the equation discussed in the previous paragraph becomes just M(R). Furthermore, by (iii), the two remaining factors in the first term on the right hand side are precisely  $M(R^+)$  and  $M(R^-)$ . Finally, by (iv), the two remaining factors in the second term on the right hand side are precisely  $M(R^+)$  and  $M(R^-)$ . Thus, the equation at which we have arrived is precisely (4), and the

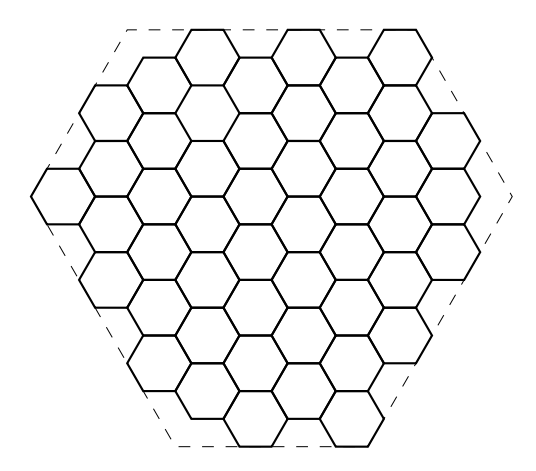


Figure 9: The (a, b)-benzel for a = 7, b = 8.

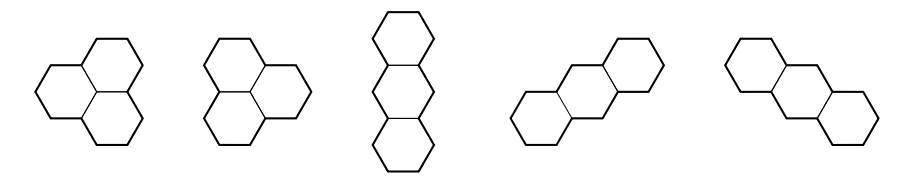


Figure 10: Left stone, right stone, vertical bone, rising bone, and falling bone (left to right).

proof is complete.  $\Box$ 

# 3 Solution of Four Open Problems of Propp

In this section we solve four open problems posed by Propp [30] on the enumeration of trimer coverings of regions called benzels. To state the problems, we first define the benzel regions. For any positive integers a and b such that  $2 \le a \le 2b$  and  $2 \le b \le 2a$ , we defined the (a, b)-benzel as follows. Consider a hexagonal grid on the plane consisting of regular hexagons of side-length 1, each having two horizontal sides (see Figure 9; this can be thought of as a tessellation of the plane by unit hexagons). We call these unit hexagons cells. Regard the plane as the complex plane so that the origin is the left vertex of one of the cells. Let H be the hexagon whose vertices are  $\omega^j(a\omega + b)$  and  $-\omega^j(a + b\omega)$  for  $j \in \{0, 1, 2\}$ , where  $\omega = e^{2\pi i/3}$ . The (a, b)-benzel is defined to be the union of all the cells that are contained in the hexagon H; Figure 9 shows the (7, 8)-benzel.

Propp considered tilings of the benzel using the following two types of tiles. A *stone* is the union of three cells that are pairwise adjacent. A *bone* is the union of three contiguous cells whose centers are collinear. Taking orientation into account, there are five different types of tiles: the *left stone*, the *right stone*, the *vertical bone*, the *rising bone*, and the *falling bone* (see Figure 10). Given a benzel, a *trimer cover* of the region is a collection

of stones and bones that covers the region without gaps or overlaps. By considering various restrictions on what tiles are allowed to be used, and the fact that the detailed shape of the (a, b)-benzel depends on the residues of a and b modulo 3, Propp was led to twenty open problems, stated in [30]. Some of these conjecture either explicit formulas or explicit recurrences for the number of trimer covers, while others concern combinatorial, respectively number theoretic properties of these numbers.

One example is: "How many trimer covers does the (a,b)-benzel have, in which all the three types of bones, but not both types of stones are allowed?" (Problem 3 in [30]). See [13] [14] [20] for recent progress on some of these problems. The open problems that we solve in this section are about the enumeration of trimer covers of benzels that can use both kinds of stones, the rising bone and the falling bone (in other words, the only restriction is that they cannot use any vertical bone). In this paper, we call such tilings vertical-bone-free tilings. Based on numerical data, Propp conjectured that the number of such trimer covers of the (3n,3n)-benzel (Problem 8), the (3n+1,3n+1)-benzel (Problem 9), the (3n+1,3n+2)-benzel (Problem 10), and the (3n-1,3n)-benzel (Problem 11) satisfy explicit recurrence relations. Proving such statements is in principle very hard, as, in contrast to the situation of dimer coverings, there are not many enumeration techniques available for trimer covers.

Recently, Defant et al. [13] found a very useful bijection, which they call *compression*, allowing one to convert trimer enumeration problems into dimer enumeration problems (see Section 3 in [13] for more details about this bijection). This opens up the possibility of proving some of Propp's conjectures using dimer enumeration techniques. We now introduce four families of regions whose domino tiling enumeration (equivalently, perfect matching enumeration of their planar dual graphs) are equivalent, thanks to the results in [13], to Problems 8–11 from Propp's list.

Recall that for a positive integer n, the Aztec diamond of order n, denoted  $AD_n$ , is the region consisting of all the unit squares on  $\mathbb{Z}^2$  whose centers (x, y) satisfy the inequality  $|x| + |y| \leq n$  (Figure 11 illustrates the Aztec diamond of order 7).

The four families of regions mentioned above, which we denote by  $TAD_{2n-1}$ ,  $TAD_{2n}$ ,  $TAD'_{2n-1}$ ,  $TAD'_{2n}$ , are simple truncations of the Aztec diamonds, obtained as follows.

To obtain the region  $TAD_{2n-1}$ , start with the Aztec diamond  $AD_{2n-1}$ , and consider the lattice point P on its southwestern boundary which lies on its southwest-to-northeast going symmetry axis. The portion of  $AD_{2n-1}$  contained in the "northeast quadrant" centered at P is the region  $TAD_{2n-1}$  (the top left picture in Figure 12 shows  $TAD_7$ ). The region  $TAD_{2n}$  is defined in the same way, starting with  $AD_{2n}$  ( $TAD_8$  is shown on the top right of Figure 12); the reason we consider separately the cases of even and odd indices is because the details of their boundaries are slightly different, and this will be reflected in their tiling enumeration formulas.

The region  $TAD'_{2n-1}$  is defined almost exactly like  $TAD_{2n-1}$ , with the one difference that the boundary lattice point from which the above-described truncation is performed is not the point P that lies on the southwest-to-northeast going symmetry axis, but is chosen instead to be the boundary point P' which is one unit step north of P (the bottom left picture in Figure 12 illustrates  $TAD'_7$ ). Similarly, the only difference between  $TAD'_{2n}$ 

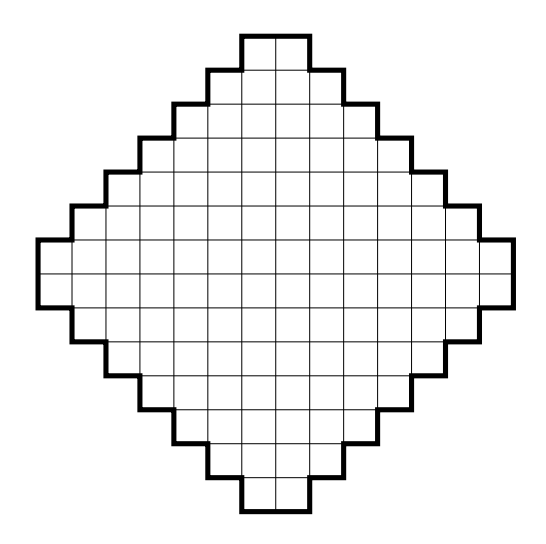


Figure 11: Aztec diamond  $AD_n$  for n = 7.

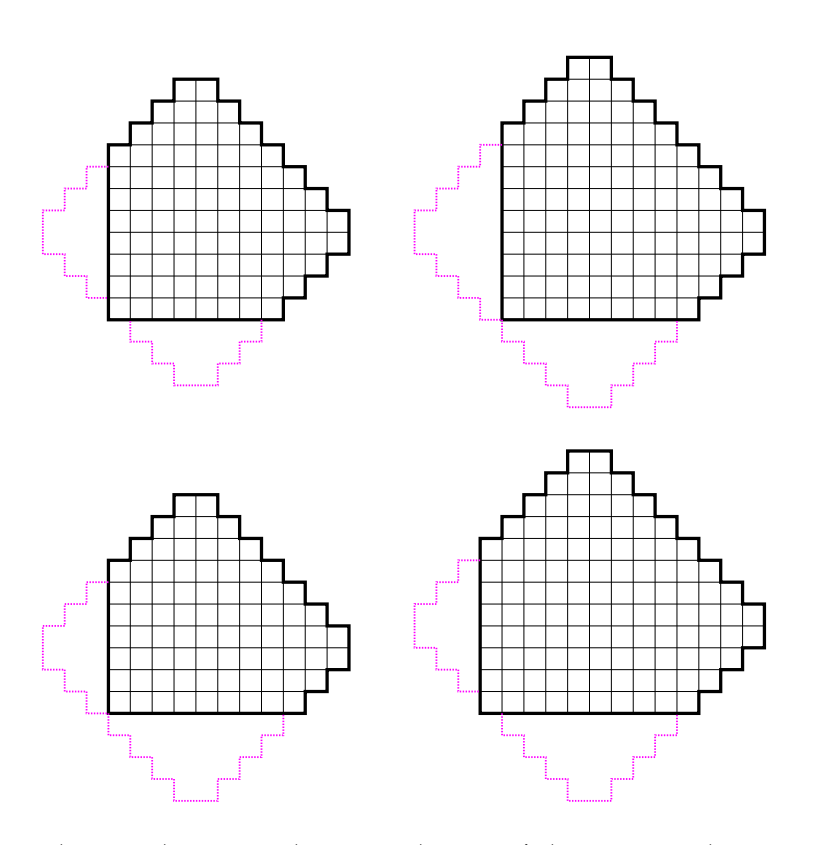


Figure 12:  $TAD_7$  (top left),  $TAD_8$  (top right),  $TAD_7$  (bottom left), and  $TAD_8$  (bottom right).

and  $TAD_{2n}$  is that for the former the truncation of  $AD_{2n}$  is not performed from P, but from the lattice point which is one unit step west of P; the bottom right picture in Figure 12 illustrates  $TAD'_8$ .

In [13] Defant et al. proved that the trimer enumeration questions in Problems 8–11 on Propp's list can be restated in terms of domino tilings of truncated Aztec diamonds as follows<sup>11</sup> (see Conjectures 5.1–5.3 and Question 5.4 in [13]).

**Theorem 4** (Defant et al. [13]). Let n be a positive integer.

- (a). The number of vertical-bone-free tilings of the (3n, 3n)-benzel is  $M(TAD_{2n-1})$ .
- (b). The number of vertical-bone-free tilings of the (3n+1,3n+1)-benzel is  $M(TAD_{2n})$ .
- (c). The number of vertical-bone-free tilings of the (3n-1,3n)-benzel is  $M(TAD'_{2n-1})$ .
- (d). The number of vertical-bone-free tilings of the (3n+1,3n+2)-benzel is  $M(TAD'_{2n})$ .

Thus, to prove Propp's original conjectures, it suffices to enumerate the domino tilings of  $TAD_{2n-1}$ ,  $TAD_{2n}$ ,  $TAD'_{2n-1}$ , and  $TAD'_{2n}$ . The main result of this section, Theorem 5 below, provides explicit, simple product formulas for the number of domino tilings of these regions.

**Theorem 5.** For positive integers n, the numbers of domino tilings of the four regions  $TAD_{2n-1}$ ,  $TAD_{2n}$ ,  $TAD_{2n-1}$ , and  $TAD_{2n}$  are given by the following product formulas<sup>12</sup>:

$$M(TAD_{2n-1}) = 2^{n^2} \cdot \frac{(2n-1)!!}{n!} \cdot \prod_{i=1}^{2n-1} \frac{(2i)!}{(n+i)!},$$
(6)

$$M(TAD_{2n}) = 2^{n(n+1)} \cdot \prod_{i=0}^{n-1} \frac{(4i+2)!(4i+3)!}{(n+2i+1)!(n+2i+2)!},$$
(7)

$$M(TAD'_{2n-1}) = 2^{n^2 - 1} \cdot \prod_{i=0}^{n-1} \frac{(4i+2)!}{(n+2i+1)!} \cdot \prod_{i=0}^{n-2} \frac{(4i+3)!}{(n+2i+1)!},$$
 (8)

and

$$M(TAD'_{2n}) = 2^{n(n+1)} \cdot \frac{(2n+1)!!}{(n+1)!} \cdot \prod_{i=0}^{n-1} \frac{(4i+2)!(4i+4)!}{(n+2i+1)!(n+2i+3)!}.$$
 (9)

Corollary 6. Let n be a positive integer.

- (a). The number of vertical-bone-free tilings of the (3n, 3n)-benzel is given by (6).
- (b). The number of vertical-bone-free tilings of the (3n + 1, 3n + 1)-benzel is given by (7).
  - (c). The number of vertical-bone-free tilings of the (3n-1,3n)-benzel is given by (8).
- (d). The number of vertical-bone-free tilings of the (3n + 1, 3n + 2)-benzel is given by (9).

<sup>&</sup>lt;sup>11</sup>For a lattice region R on the square lattice, M(R) denotes the number of its domino tilings.

<sup>&</sup>lt;sup>12</sup>Throughout this paper, an empty product is defined to be 1 and  $(2m-1)!! := (2m-1)(2m-3)\cdots 1$  for postive integers m.

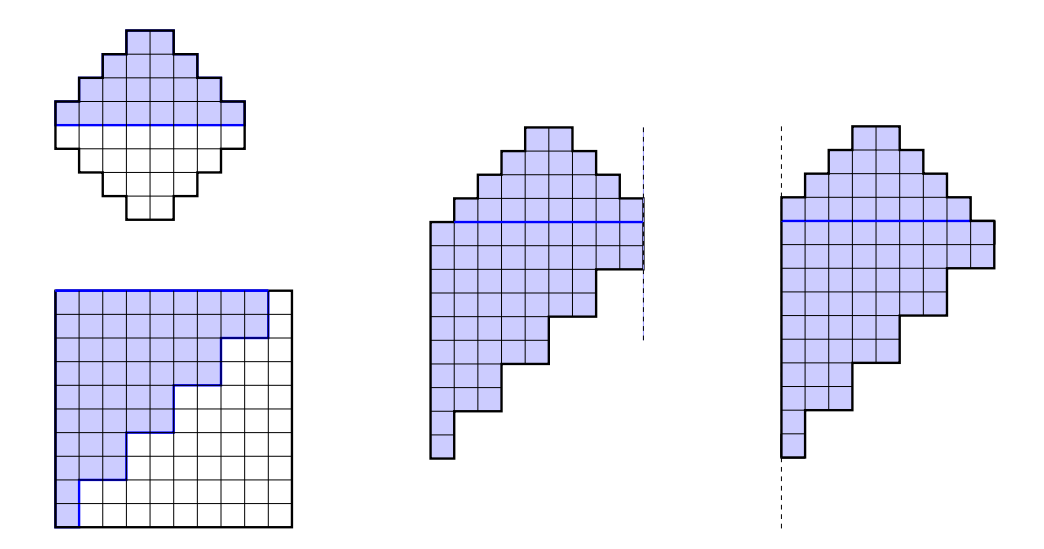


Figure 13: Using half of  $AD_{n-1}$  and half of the square  $S_{2n}$  (left) to get the Aztec triangles  $\mathcal{T}_n$  (center) and  $\mathcal{T}'_n$  (right), for n=5.

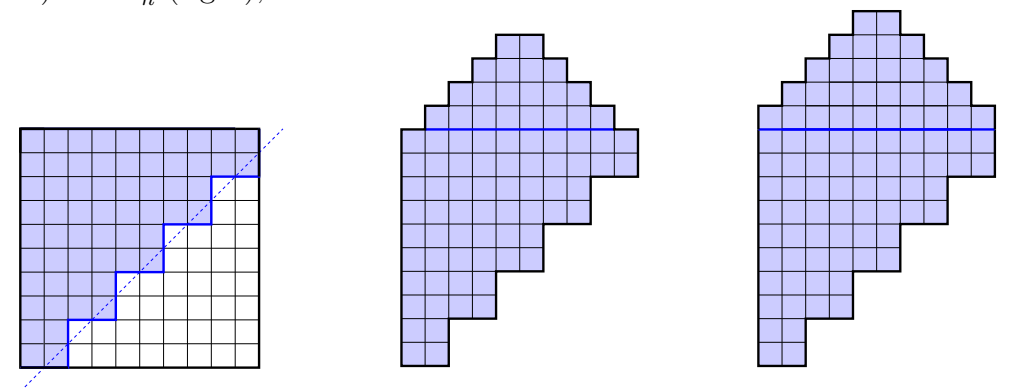


Figure 14: Using an augmented half of the square  $S_{2n}$  (left) and half of  $AD_{n-1}$  to get the Aztec triangle  $\mathcal{T}''_n$  (center), and the same augmented half of the square  $S_{2n}$ , but together with half of  $AD_n$ , to obtain the Aztec triangle  $\mathcal{T}'''_{n+1}$  (right), for n = 5.

The proof of Theorem 5 is based on Theorem 1(a) (for (6) and (7)), Theorem 1(b) (for (8) and (9)), and some enumeration results of Corteel et al. presented in [12]. As a result of applying Theorem 1, four new families of regions arise.

One of these families consists of the Aztec triangles introduced by Di Francesco [15], and the remaining three are variants of it. All of them can be regarded as hybrids between Aztec diamonds and squares. Namely, let  $S_{2n}$  be the square of side-length 2n drawn on the square grid. Cut it in two congruent parts<sup>13</sup> by a zig-zag lattice path of step length 2n, as shown in Figure 13, and glue together the top half with the top half of  $AD_{n-1}$ . If this is done in a right-justified manner, one obtains Di Francesco's Aztec triangle  $\mathcal{T}_n$  (see the picture in the center in Figure 13); the left-justified fashion results in the Aztec triangle

<sup>&</sup>lt;sup>13</sup>This way of cutting up the square appears also in the second author's paper [4] and in Pachter's work [29].

 $\mathcal{T}'_n$  (see the picture on the right in Figure 13).

To obtain the remaining two variants, use the "augmented half" of the square  $S_{2n}$  obtained by cutting  $S_{2n}$  with the translation of the above zig-zag cut one unit square diagonal in the southeast direction (see the picture on the left in Figure 14). Gluing the top half of  $AD_{n-1}$  to this augmented half results in the Aztec triangle  $\mathcal{T}''_n$  (see the picture in the center in Figure 14), while gluing the top half of  $AD_n$  to it produces the Aztec triangle  $\mathcal{T}'''_{n+1}$  (see the picture on the right in Figure 14). Note that for all the four variants, the order of the Aztec triangle is one more than the order of the Aztec diamond whose top half was used to construct it.

We will find it convenient to have the indexing of the regions in the last family shifted by one unit, as in the above definition. But due to this, we need to define  $\mathcal{T}_1'''$  separately: we set  $\mathcal{T}_1'''$  to be the empty region, which has one domino tiling (the empty set of dominos).

These four families of regions turn out to be special cases of regions considered by Corteel et al. in [12]. In that paper, the authors consider a family of regions parametrized by positive integers l and k. The region  $\mathcal{T}_n$  represents the special case l=2n and k=n. Furthermore,  $\mathcal{T}'_n$  is the special case l=2n+1 and k=n-1,  $\mathcal{T}''_n$  the special case l=2n+1 and k=n, and  $\mathcal{T}'''_n$  is obtained by setting l=2n and k=n-1.

By specializing the values of l and k in Theorem 1.2 of [12] as indicated in the previous paragraph, we obtain the following enumeration results for the number of domino tilings of these four families of regions.

**Lemma 7.** For positive integers n, the number of domino tilings of the four types of Aztec triangles is given by

$$M(\mathcal{T}_n) = M(\mathcal{T}'_n) = 2^{n(n-1)/2} \cdot \prod_{i=0}^{n-1} \frac{(4i+2)!}{(n+2i+1)!},$$
(10)

$$M(\mathcal{T}_n'') = 2^{n(n+1)/2} \cdot \prod_{i=0}^{n-1} \frac{(4i+3)!}{(n+2i+2)!},$$
(11)

and

$$M(\mathcal{T}_n''') = 2^{n(n-1)/2} \cdot \frac{(2n-1)!!}{n!} \cdot \prod_{i=1}^{n-1} \frac{(4i)!}{(n+2i)!}.$$
 (12)

The equality  $M(\mathcal{T}_n) = M(\mathcal{T}'_n)$  was proved by Corteel et al. in [12] by showing that the two numbers are given by the same formula. Recently, a bijective proof was given in [2] by the first two authors of the current paper.

Proof of Theorem 5. The first two equalities (6) and (7) turn out to be direct consequences of the factorization theorem for perfect matchings (Theorem 1(a)) and the specializations of [12, Theorem 1.2] stated in Lemma 7. Indeed, note that the regions  $TAD_{2n-1}$  and  $TAD_{2n}$  are symmetric. If we apply the factorization theorem to their planar duals, we get, after removing some forced dominos (see Figure 15)

$$M(TAD_{2n-1}) = 2^n M(\mathcal{T}_n) M(\mathcal{T}_n'''), \tag{13}$$

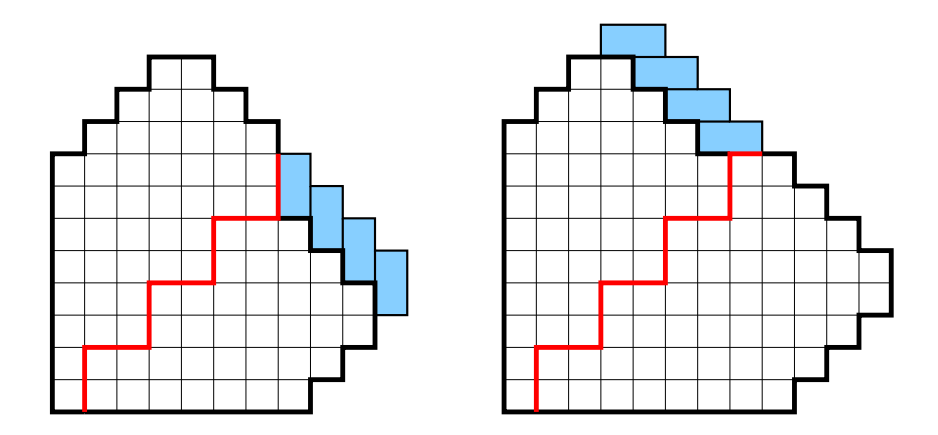


Figure 15: Left. Factorization of  $TAD_7$  into  $\mathcal{T}_4$  and  $\mathcal{T}_4'''$ . Right. Factorization of  $TAD_8$  into  $\mathcal{T}_4'$  and  $\mathcal{T}_4'''$ .

and

$$M(TAD_{2n}) = 2^n M(\mathcal{T}'_n) M(\mathcal{T}''_n). \tag{14}$$

The situation is different for the regions  $TAD'_{2n-1}$  and  $TAD'_{2n}$ , as they are not symmetric. To apply Theorem 1(b), we first "symmetrize" these regions about their diagonals; denote by  $\overline{TAD'}_{2n-1}$  and  $\overline{TAD'}_{2n}$ , respectively, the resulting symmetric regions (in Figure 16, these are the regions enclosed by the outermost contours). These new regions have no domino tilings, as they have an odd number of vertices. Let v be the rightmost unit square in the top row of these regions (v is colored black in Figure 16). Since after removing the forced dominos from  $\overline{TAD'}_{2n-1} \setminus v$  one obtains the region  $\overline{TAD'}_{2n-1}$ , these two regions have the same number of tilings. The same is true for the regions  $\overline{TAD'}_{2n} \setminus v$  and  $\overline{TAD'}_{2n} \setminus v$  are symmetric graphs with a boundary defect, so we can apply Theorem 1(b) to them. Applying it we get (after removing the forced dominos; see Figure 16)

$$M(TAD'_{2n-1}) = M(\overline{TAD'}_{2n-1} \setminus v) = 2^{n-1} M(\mathcal{T}''_{n-1}) M(\mathcal{T}''_n), \tag{15}$$

and

$$M(TAD'_{2n}) = M(\overline{TAD'}_{2n} \setminus v) = 2^n M(\mathcal{T}_n) M(\mathcal{T}'''_{n+1}).$$
(16)

It is straightforward to check that one gets expressions (6)–(9) by combining equations (10)–(12) and (13)–(16). This completes the proof.

Remark 2. The original conjectures of Propp did not state explicit formulas for the number of vertical-bone-free tilings of benzels. Instead, the conjectures stated that those numbers satisfy certain recurrence relations. More precisely, via the compression bijection of [13], Propp's conjectures (open Problems 8–11 in [30]) are equivalent to the following equalities ((17) and (20) were given in [30] and the other two in [13]):

$$\frac{M(TAD_{2n-1})M(TAD_{2n+3})}{M(TAD_{2n+1})^2} = \frac{256(2n+3)^2(4n+1)(4n+3)^2(4n+5)}{27(3n+1)(3n+2)^2(3n+4)^2(3n+5)}$$
(17)

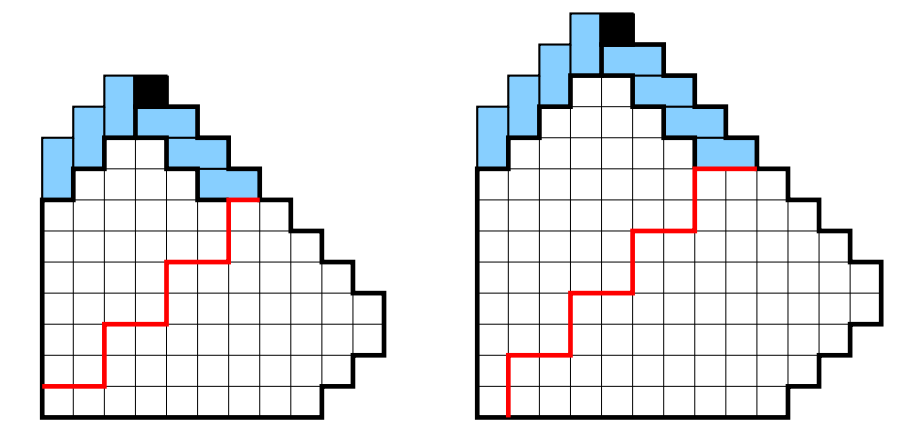


Figure 16: Factorization of  $\overline{TAD'}_7 \setminus v$  into  $\mathcal{T}_3''$  and  $\mathcal{T}_4'$  (left) and that of  $\overline{TAD'}_8 \setminus v$  into  $\mathcal{T}_4$  and  $\mathcal{T}_5'''$  (right); v is indicated by a black unit square.

for all  $n \ge 1$ ,

$$\frac{M(TAD_{2n})}{M(TAD_{2n-2})} = \frac{2^{2n}(4n-1)!(4n-2)!n!}{(3n)!(3n-1)!(3n-2)!}$$
(18)

for all  $n \ge 2$ ,

$$\frac{M(TAD'_{2n-1})}{M(TAD'_{2n-3})} = \frac{2^{2n-3}(4n-2)!(4n-4)!(n-1)!!(n-3)!!}{(3n-1)!!(3n-2)!(3n-3)!(3n-5)!!}$$
(19)

for all  $n \ge 2$ , and

$$= \frac{\frac{M(TAD'_{2n}) M(TAD'_{2n+6})}{M(TAD'_{2n+2}) M(TAD'_{2n+4})}}{729(3n+2)(3n+4)^2(3n+5)^2(3n+7)^2(3n+8)^2(3n+10)}$$
(20)

for all  $n \ge 1$ . It is straightforward to check that formulas (6)-(9) satisfy the above equalities (17)-(20); thus Corollary 6 indeed solves the four open problems of Propp.

Note also that deducing the simple product formulas (6)–(9) directly from the above recurrences would not be an easy task.

### 4 Nearly symmetric hexagons with collinear holes

In this section we solve an open problem posed by Lai — namely, Problem 28 in [24] — by providing an explicit product formula for the number of lozenge tilings of a certain family of hexagonal regions with holes on the triangular lattice (the regions  $H'_1(a, b, k)$ ; see subsection 4.1 and Theorems 10(a) and 11(a)). This family is closely related to one of three families of symmetric hexagonal regions with collinear triangular holes (the regions  $H_1(a, b, k)$ , also described in subsection 4.1) whose number of lozenge tilings was

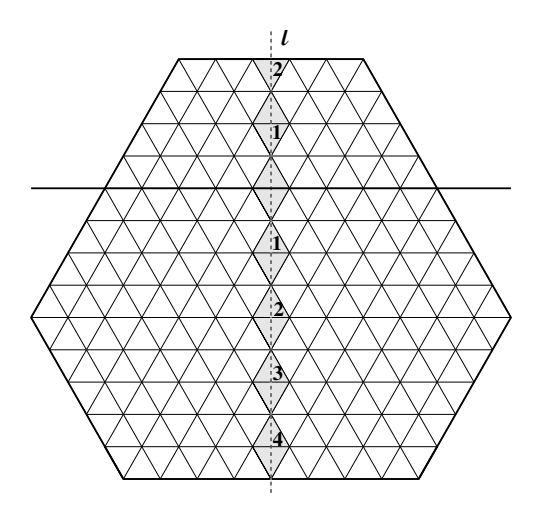


Figure 17: The labeling of the slots along a vertical line, starting from a reference horizontal lattice line; slots that are only partially contained in H are also labeled.

determined in [5] by the second author of the current paper: it is obtained from the latter by translating all the holes one unit in the southeast lattice direction. In addition to solving Lai's open problem, we also provide explicit product formulas for two more families of regions, obtained from the two remaining families from [5] by the same procedure; see Theorems 10(b)(c) and 11(b)(c).

#### 4.1 Six families of hexagonal regions with collinear holes

We now recall the definitions of the three families of regions  $H_{\mathbf{l}}(a,b,k)$ ,  $H_{\mathbf{l},\mathbf{q}}(a,b,k)$  and  $\bar{H}_{\mathbf{l},\mathbf{q}}(a,b,k)$  introduced in [5]; the other three families,  $H'_{\mathbf{l}}(a,b,k)$ ,  $H'_{\mathbf{l},\mathbf{q}}(a,b,k)$  and  $\bar{H}'_{\mathbf{l},\mathbf{q}}(a,b,k)$  are defined by a simple variation of these.

Draw the triangular lattice so that one of the families of lattice lines is horizontal, and let H be a hexagon on this lattice. Let  $\ell$  be a vertical line containing lattice points and crossing the interior of H. A slot is the union of two unit triangles crossed by  $\ell$  which share an edge. Essential in the definition of our regions is the concept of labeling the slots contained in H, starting from a reference horizontal lattice line L. This is very simple: label the slots on both sides of L successively by  $1, 2, 3, \ldots$  (the two closest ones by 1, the next two by 2, and so on), including also any slots that are only partially contained in H; this is illustrated in Figure 17.

Given non-negative integers a, b and k, denote by H(a, b, k) the hexagonal region on the triangular lattice whose side-lengths are a, b+k, b, a+k, b, b+k, clockwise from top. Thus H(a, b, k) has k more up-pointing unit triangles than down-pointing unit triangles. Our regions will be obtained from H(a, b, k) by making some holes in it, so that the union of the holes has k more up- than down-pointing triangles; this way, the resulting regions will have the same number of unit triangles of the two kinds, a necessary condition for the existence of lozenge tilings.

Let  $\ell$  be the vertical symmetry axis of H(a,b,k), and label the slots along  $\ell$  choosing

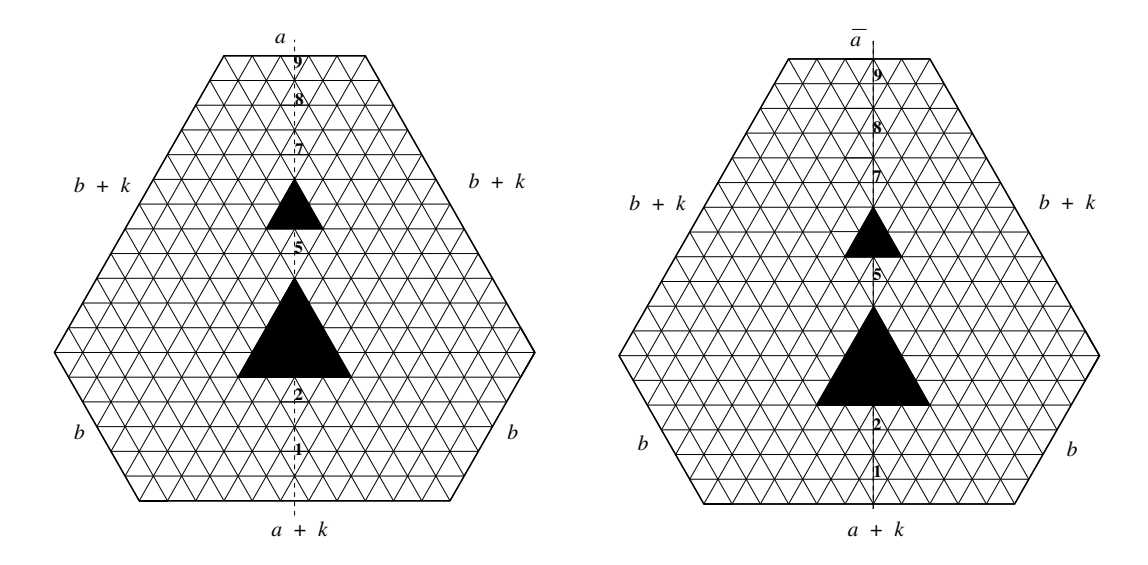


Figure 18: Left. The symmetric hexagon with holes  $H_{\mathbf{l}}(a,b,k)$  for a=5, b=6, k=6, and  $\mathbf{l}=(1,2,5,7,8,9)$ . Right. The corresponding nearly symmetric hexagon with holes  $H'_{\mathbf{l}}(a,b,k)$  for a=5, b=6, k=6, and  $\mathbf{l}=(1,2,5,7,8,9)$ .

the reference line L to be the base of H(a,b,k) (see the picture on the left in Figure 18 for an example). Choose an arbitrary subset of the labeled slots along  $\ell$  (avoiding the possible partial slot at the top), and for each chosen slot remove the up-pointing lattice triangle of side-length two containing that slot. If the resulting region has forced lozenges, remove them<sup>14</sup>. Let  $\mathbf{l}$  be the list of the labels of slots not covered by removed triangles in the resulting region. Then we denote the resulting region by  $H_{\mathbf{l}}(a,b,k)$ ; an example is shown on the left in Figure 18.

The regions  $H'_1(a, b, k)$  featured in Lai's open problem that we solve in this section are defined very similarly. Indeed, the only difference is that instead of the symmetry axis  $\ell$ , we consider its translation  $\ell'$  half a unit to the right, and we label the slots along  $\ell'$ , with the reference line still being the base of H(a, b, k). Letting I be the list of slot labels not covered by the removed triangles, the resulting region is defined to be  $H'_1(a, b, k)$  (see the picture on the right in Figure 18 for an example). Lai noticed, based on data, that the number of lozenge tilings of these regions always seems to factor into relatively small prime factors, a fact that points to the existence of a simple product formula. In [24, Problem 28] he posed the open problem of finding and proving such a formula. We provide this in Theorem 10(a). Furthermore, in Theorem 10(b) we give simple product formulas for the number of tilings of two more families of regions, namely the regions  $H'_{1,\mathbf{q}}(a,b,k)$  and  $\bar{H}'_{1,\mathbf{q}}(a,b,k)$  defined below.

The main new ingredient in the last two pairs of families of regions is that their definition also involves making one triangular hole of odd side-length. More precisely, let the

<sup>&</sup>lt;sup>14</sup>By this, if a run of k triangular holes of side-length two are contiguous, this gets replaced by a single triangular hole of side-length 2k. In addition, it follows that the top triangular hole in  $H_1(a, b, k)$  does not touch the top side of the boundary.

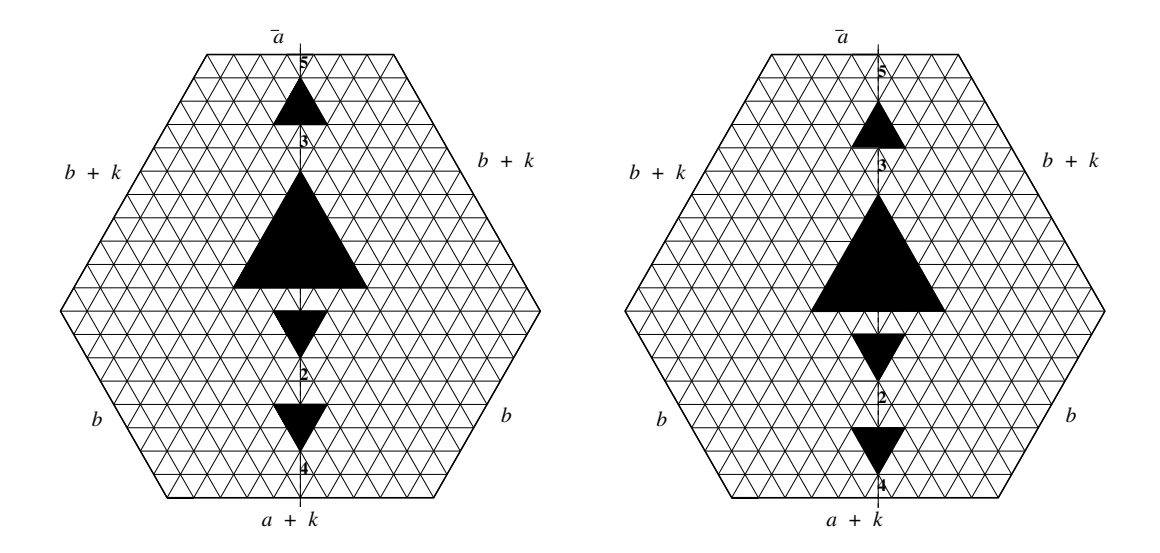


Figure 19: Left. The symmetric hexagon with holes  $H_{\mathbf{l},\mathbf{q}}(a,b,k)$  for  $a=7,\ b=8,\ k=3,$   $\mathbf{l}=(2,4)$  and  $\mathbf{q}=(3,5)$ . Right. The corresponding nearly symmetric hexagon with holes  $H'_{\mathbf{l},\mathbf{q}}(a,b,k)$  for  $a=7,\ b=8,\ k=3,\ \mathbf{l}=(2,4)$  and  $\mathbf{q}=(3,5)$ .

reference line L be a horizontal lattice line that meets the region H(a,b,k), and consider again the symmetry axis  $\ell$ . Label the slots along  $\ell$  with L as the reference line, and remove an up-pointing triangle of odd size, symmetrically about  $\ell$ , whose base is along L. Then, as for the previous family, choose arbitrarily some labeled slots — now generating two subsets of labels, one for slots below L and one for those above L. Then remove triangles of side two straddling the chosen slots, with an important difference: for the slots above L, choose them to be up-pointing, but for the slots below L make them down-pointing. Use the same convention about removing any forced lozenges. If in the resulting region the leftover labels below L form the list  $\mathbf{l}$ , and those above L the list  $\mathbf{q}$ , we define the resulting region to be  $H_{\mathbf{l},\mathbf{q}}(a,b,k)$ ; an example is illustrated on the left in Figure 19. We define the region  $H'_{\mathbf{l},\mathbf{q}}(a,b,k)$  by applying exactly the same procedure, but with  $\ell$  replaced by its half-unit translation to the right,  $\ell'$ ; see the picture on the right in Figure 19 for an example.

The last pair of families of regions is very similar to the previous one; the only difference is that the triangular hole of odd side-length is chosen to point  $downward^{15}$ . We denote the resulting regions by  $\bar{H}_{\mathbf{l},\mathbf{q}}(a,b,k)$  and  $\bar{H}'_{\mathbf{l},\mathbf{q}}(a,b,k)$ , respectively (these are illustrated in Figure 20).

#### 4.2 Two families of dented regions

We recall here the definitions of two more families of regions whose lozenge tilings were enumerated in [5]; they will be essential for solving Lai's open problem. The detailed

<sup>&</sup>lt;sup>15</sup>Note that such a region cannot be obtained by rotating an  $H_{1,\mathbf{q}}(a,b,k)$  by 180°, because we are assuming that k, which is the difference between the number of up-pointing and down-pointing unit triangles in H(a,b,k), is non-negative.

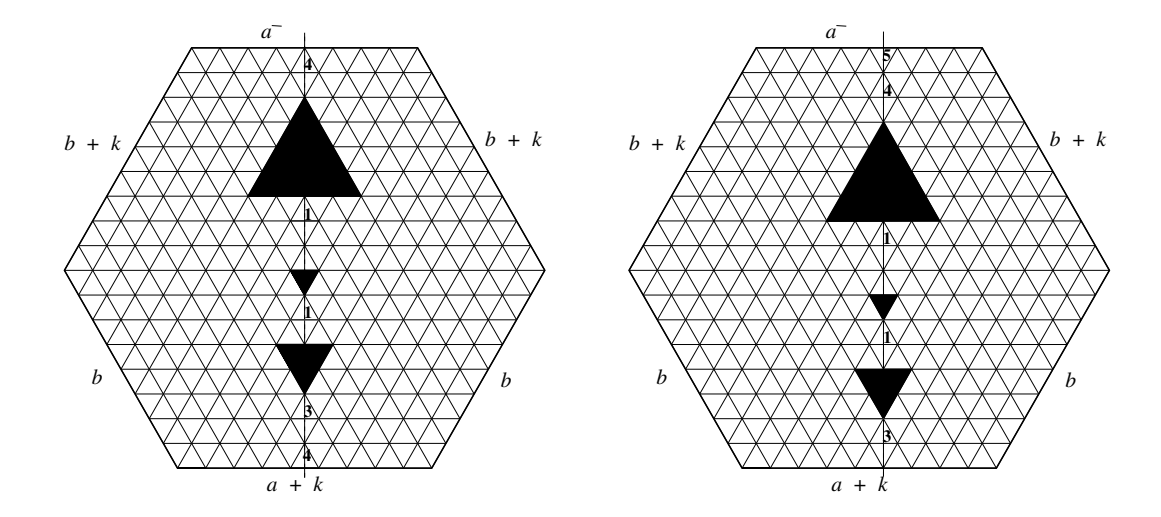


Figure 20: Left. The symmetric hexagon with holes  $\bar{H}_{\mathbf{l},\mathbf{q}}(a,b,k)$  for  $a=b=8,\ k=1,$   $\mathbf{l}=(1,3,4)$  and  $\mathbf{q}=(1,4)$ . Right. The corresponding nearly symmetric hexagon with holes  $\bar{H}'_{\mathbf{l},\mathbf{q}}(a,b,k)$  for  $a=b=8,\ k=1,\ \mathbf{l}=(1,3)$  and  $\mathbf{q}=(1,4,5)$ .

definitions are given in [5]; we rely here on Figures 21–24 to define our regions.

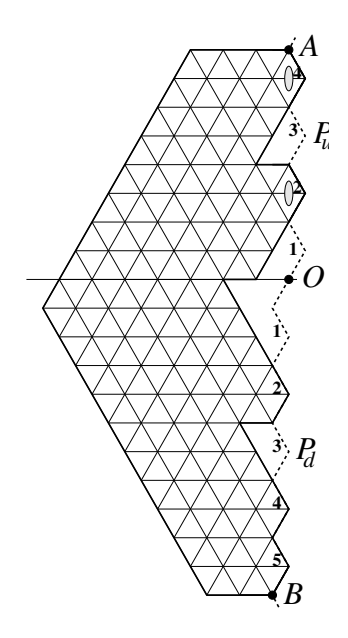
Consider two semi-infinite vertical zigzag paths  $P_u$  and  $P_d$ , meeting at the reference point O as shown in Figure 21 (in that figure,  $P_u$  connects O to A, while  $P_b$  connects O to B). Label the slots that fit in their folds (call these bumps) as shown in the figure. The tile positions corresponding to the bumps above O are weighted by 1/2 (this is indicated by shaded ellipses in the figures).

Given non-empty lists of strictly increasing positive integers  $\mathbf{l} = (l_1, \dots, l_m)$  and  $\mathbf{q} = (q_1, \dots, q_n)$  and a non-negative integer x, the region  $R_{\mathbf{l},\mathbf{q}}(x)$  is defined as indicated in Figure 21. The lists  $\mathbf{l}$  and  $\mathbf{q}$  specify which bumps on the zigzag lines are kept. The kept bumps on  $P_u$  are joined together by creating up-pointing dents, and those on  $P_d$  by down-pointing dents; these two portions are then joined together via a horizontal ray left of O, as shown; x is the length of the base. Note that this information, together with the fact that we want a region which can be tiled by lozenges, determines the rest of the boundary of  $R_{\mathbf{l},\mathbf{q}}(x)^{16}$ .

In case one of the lists  $\mathbf{l}$  or  $\mathbf{q}$  is empty, the definition is slightly different, as shown in Figure 22; note in particular that if  $\mathbf{l} = \emptyset$ , x is not the length of the base, but one unit less than the distance from the left end of the base to the reference point O. Define  $R_{\emptyset,\emptyset}(x) = \emptyset$  for all x.

Our second family of regions, denoted  $\bar{R}_{l,q}(x)$ , is defined almost identically (see Figures 23 and 24). The only difference is that, when connecting the upper and lower boundary portions determined by the selected bumps, instead of the horizontal ray starting from O, we use the one starting from the lattice point  $\bar{O}$ , one step southwest of O (and, in case

<sup>&</sup>lt;sup>16</sup>Indeed, if a lozenge tiling exists, due to a family of paths of lozenges that it determines, the length of the southwest side must be equal to the number of unit segments facing northeast on the right boundary.



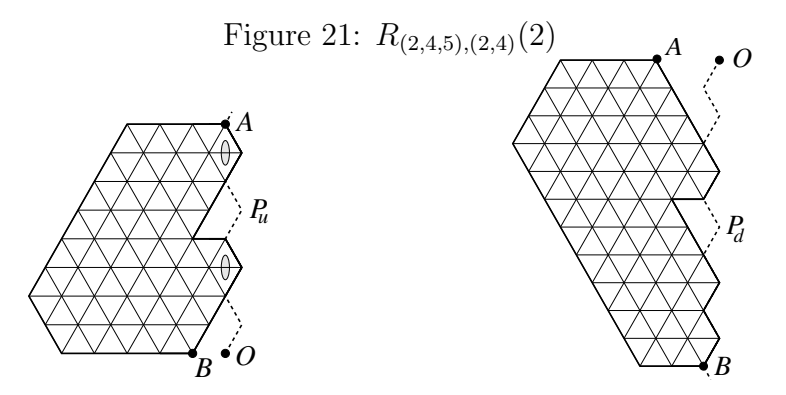


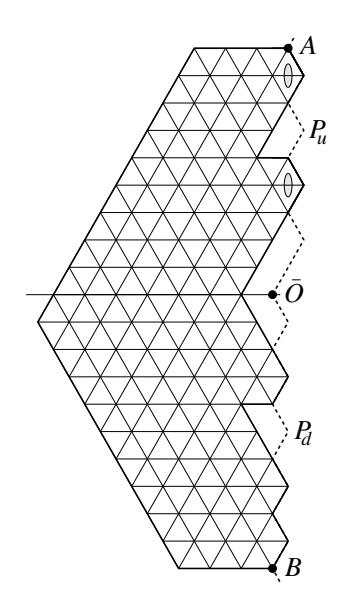
Figure 22:  $R_{\emptyset,(2,4)}(4)$  (left) and  $R_{(2,4,5),\emptyset}(2)$  (right).

**l** is empty, when defining the bottom side of  $\bar{R}_{\emptyset,\mathbf{q}}(x)$ , we move left until we are x units away from  $\bar{O}$ ). Again, we define  $\bar{R}_{\emptyset,\emptyset}(x) = \emptyset$  for all x.

#### 4.3 Two families of polynomials and their connection to the dented regions

Given integers  $m, n \ge 0$  and lists  $\mathbf{l} = (l_1, \dots, l_m)$  and  $\mathbf{q} = (q_1, \dots, q_n)$  of strictly increasing positive integers, we define the polynomials  $P_{\mathbf{l},\mathbf{q}}(x)$  and  $\overline{P}_{\mathbf{l},\mathbf{q}}(x)$  as follows.

We first define the monic polynomials  $B_{m,n}(x)$  and  $\bar{B}_{m,n}(x)$ . Recall that for any real number a and non-negative integer k, the Pochhammer symbol  $(a)_k$  is defined by setting  $(a)_0 := 1$ , and  $(a)_k := \prod_{i=1}^k (a+i-1)$  for k > 0. In addition, for a and k like above, we will find it convenient to use the notation



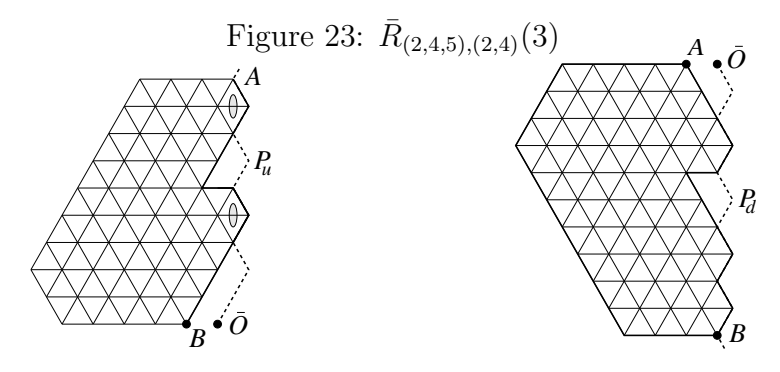


Figure 24:  $\bar{R}_{\emptyset,(2,4)}(5)$  (left) and  $\bar{R}_{(2,4,5),\emptyset}(3)$  (right).

$$\langle a, a+k \rangle := \prod_{i=0}^{k} (a+i)^{\min(i+1,k+1-i)}$$
  
=  $a(a+1)^2 \cdots (a+k-1)^2 (a+k)$   
=  $\prod_{i=0}^{\lfloor \frac{k}{2} \rfloor} (a+i)_{k+1-2i}, \quad k \geqslant 0,$ 

and  $\langle a, a + k \rangle := 1$  for k < 0.

With this notation, for non-negative integers m and n,  $B_{m,n}(x)$  and  $\bar{B}_{m,n}(x)$  are defined to be the monic polynomials given by

$$B_{m,n}(x) = 2^{-mn-m(m-1)/2} (x+n+1)_m (x+n+2)_m \langle x+2, x+n \rangle \left\langle x+\frac{3}{2}, x+\frac{2n+1}{2} \right\rangle$$

$$\times \prod_{i=1}^n \frac{(x+i)_m}{(x+i+1/2)_m} \prod_{i=1}^m (2x+n+i+2)_{n+i-1}$$

and

$$\bar{B}_{m,n}(x) = 2^{-mn-n(n+1)/2} (x+m+1)_n \langle x+1, x+m \rangle \left\langle x + \frac{3}{2}, x + \frac{2m-1}{2} \right\rangle$$

$$\times \prod_{i=1}^m \frac{(x+i)_n}{(x+i+1/2)_n} \prod_{i=1}^n (2x+m+i+1)_{m+i}.$$

Next, given lists of strictly increasing positive integers  $\mathbf{l} = (l_1, \dots, l_m)$  and  $\mathbf{q} = (q_1, \dots, q_n)$ , we define the constants  $c_{\mathbf{l},\mathbf{q}}$  and  $\bar{c}_{\mathbf{l},\mathbf{q}}$  by

$$c_{\mathbf{l},\mathbf{q}} = 2^{\binom{n-m}{2}-m} \prod_{i=1}^{m} \frac{1}{(2l_i)!} \prod_{i=1}^{n} \frac{1}{(2q_i-1)!} \frac{\prod_{1 \leq i < j \leq m} (l_j-l_i) \prod_{1 \leq i < j \leq n} (q_j-q_i)}{\prod_{i=1}^{m} \prod_{j=1}^{n} (l_i+q_j)}$$

and

$$\bar{c}_{\mathbf{l},\mathbf{q}} = 2^{\binom{n-m}{2}-m} \prod_{i=1}^{m} \frac{1}{(2l_i-1)!} \prod_{i=1}^{n} \frac{1}{(2q_i)!} \frac{\prod_{1 \leq i < j \leq m} (l_j-l_i) \prod_{1 \leq i < j \leq n} (q_j-q_i)}{\prod_{i=1}^{m} \prod_{j=1}^{n} (l_i+q_j)}.$$

We are now ready to define our polynomials  $P_{\mathbf{l},\mathbf{q}}(x)$  and  $\bar{P}_{\mathbf{l},\mathbf{q}}(x)$ . For lists of strictly increasing positive integers  $\mathbf{l} = (l_1, \ldots, l_m)$  and  $\mathbf{q} = (q_1, \ldots, q_n)$ ,  $P_{\mathbf{l},\mathbf{q}}(x)$  and  $\bar{P}_{\mathbf{l},\mathbf{q}}(x)$  are given by <sup>1718</sup>

$$P_{\mathbf{l},\mathbf{q}}(x) = c_{\mathbf{l},\mathbf{q}} B_{m,n}(x + l_m - m) \prod_{i=1}^{m} \prod_{j=i}^{l_i-1} (x + l_m - j)(x + l_m - m + n + j + 2)$$

$$\times \prod_{i=1}^{n} \prod_{j=i}^{q_i-1} (x + l_m - m + n - j + 1)(x + l_m + j + 1)$$
(21)

and

$$\bar{P}_{\mathbf{l},\mathbf{q}}(x) = \bar{c}_{\mathbf{l},\mathbf{q}}\bar{B}_{m,n}(x+l_m-m)\prod_{i=1}^{m}\prod_{j=i}^{l_i-1}(x+l_m-j)(x+l_m-m+n+j+1)$$

$$\times \prod_{i=1}^{n}\prod_{j=i}^{q_i-1}(x+l_m-m+n-j)(x+l_m+j+1).$$
(22)

In [5], the second author showed that the tiling generating functions of the regions  $R_{\mathbf{l},\mathbf{q}}(x)$  and  $\bar{R}_{\mathbf{l},\mathbf{q}}(x)$  introduced in subsection 4.2 are given by the above polynomials  $P_{\mathbf{l},\mathbf{q}}(x)$  and  $\bar{P}_{\mathbf{l},\mathbf{q}}(x)$ .

Theorem 8 (Ciucu [5]). We have

$$M(R_{\mathbf{l},\mathbf{q}}(x)) = P_{\mathbf{l},\mathbf{q}}(x) \tag{23}$$

and

$$M(\bar{R}_{\mathbf{l},\mathbf{q}}(x)) = \bar{P}_{\mathbf{l},\mathbf{q}}(x). \tag{24}$$

 $<sup>^{17}</sup>$ These are equations (5.1) and (5.2) in [5, Part B].

<sup>&</sup>lt;sup>18</sup>For m = 0, one needs to take  $l_m = 0$  in equations (21) and (22); also, when m or n is zero at the upper limit of an outside product, that double product is defined to be 1.

# 4.4 Lozenge tilings of symmetric hexagons with holes along the symmetry axis.

The number of lozenge tilings of the regions  $H_{\mathbf{l}}(a,b,k)$ ,  $H_{\mathbf{l},\mathbf{q}}(a,b,k)$ , and  $\bar{H}_{\mathbf{l},\mathbf{q}}(a,b,k)$  (three of the six families of regions introduced in subsection 4.1) was determined by the second author in [5]. The proof is based on the factorization theorem for matchings [4, Theorem 1.2] and equalities (23)–(24). The result (stated in a slightly different form) is the following.

**Theorem 9** (Theorem 1.1 in [5]). Let H be one of the regions  $H_{\mathbf{l}}(a,b,k)$ ,  $H_{\mathbf{l},\mathbf{q}}(a,b,k)$  or  $\bar{H}_{\mathbf{l},\mathbf{q}}(a,b,k)$ . Then we have<sup>19</sup>

$$M(H) = 2^{w_{\ell}(H)} M(H^{+}) M(H^{-}),$$
 (25)

and all of the regions  $H^+$  and  $H^-$  are R- or  $\bar{R}$ -regions, as follows  $^{20}$ :

(a). For k even, we have

$$[H_{\mathbf{l}}(a,b,k)^{+},H_{\mathbf{l}}(a,b,k)^{-}] = \begin{cases} [\bar{R}_{\mathbf{l}-1,\emptyset}(a/2),R_{\emptyset,\mathbf{l}}((a+k-2)/2)], & a \ even, \ l_{1} = 1, \\ [R_{\mathbf{l}-1,\emptyset}(a/2),R_{\emptyset,\mathbf{l}}((a+k-2)/2)], & a \ even, \ l_{1} > 1, \\ [\bar{R}_{\mathbf{l},\emptyset}((a-1)/2),R_{\emptyset,\mathbf{l}^{(m)}}((a+k-1)/2)], & a \ odd, \end{cases}$$

$$(26)$$

where l-1 denotes the list obtained from l by decrementing each of its elements by one unit (discarding the first element if  $l_1 = 1$ ).

(b). For k odd, we have

$$[H_{\mathbf{l},\mathbf{q}}(a,b,k)^{+},H_{\mathbf{l},\mathbf{q}}(a,b,k)^{-}] = \begin{cases} [R_{\mathbf{q},\mathbf{l}^{(m)}}(a/2),\bar{R}_{\mathbf{l},\mathbf{q}}((a+k-1)/2)], & a \text{ even,} \\ [R_{\mathbf{q},\mathbf{l}}((a-1)/2),\bar{R}_{\mathbf{l},\mathbf{q}^{(n)}}((a+k)/2)], & a \text{ odd,} \end{cases}$$
(27)

and

$$[\bar{H}_{\mathbf{l},\mathbf{q}}(a,b,k)^{+},\bar{H}_{\mathbf{l},\mathbf{q}}(a,b,k)^{-}] = \begin{cases} [\bar{R}_{\mathbf{q},\mathbf{l}^{(m)}}(a/2),R_{\mathbf{l},\mathbf{q}}((a+k-1)/2)], & a \text{ even,} \\ [\bar{R}_{\mathbf{q},\mathbf{l}}((a-1)/2),R_{\mathbf{l},\mathbf{q}^{(n)}}((a+k)/2)], & a \text{ odd,} \end{cases}$$
(28)

where  $\mathbf{l}^{(k)}$  denotes the list obtained from  $\mathbf{l}^{(k)}$  by discarding its kth element.

#### 4.5 Shifting the holes one unit southeast.

The first part of the following result, together with equations (23) and (24), provides a simple product formula for the number of lozenge tilings of the region  $H'_{\mathbf{l}}(a,b,k)$  — thus solving Lai's open problem mentioned in subsection 4.1 — while the second part gives analogous formulas for the regions  $H'_{\mathbf{l},\mathbf{q}}(a,b,k)$  and  $\bar{H}'_{\mathbf{l},\mathbf{q}}(a,b,k)$ .

 $<sup>^{19}\</sup>mathrm{Here}\ H^+$  and  $H^-$  are the regions obtained from the symmetric region H by the procedure described before the statement of Theorem 1.

<sup>&</sup>lt;sup>20</sup>Given two regions R and Q, [R,Q] is the (ordered) list consisting of these regions.

**Theorem 10.** Let H be one of the regions  $H'_{\mathbf{l}}(a,b,k)$ ,  $H'_{\mathbf{l},\mathbf{q}}(a,b,k)$  or  $\bar{H}'_{\mathbf{l},\mathbf{q}}(a,b,k)$ , and let  $\ell'$  be the axis with respect to which the holes in H are symmetric. Then we have<sup>21</sup>

$$M(H) = \begin{cases} \frac{a+b+k}{a+2b+k} \cdot 2^{w_{\ell'}(H)} M(H^{+}) M(H^{-}), & a \text{ odd,} \\ \frac{a+b+k}{a} \cdot 2^{w_{\ell'}(H)} M(H^{+}) M(H^{-}), & a \text{ even,} \end{cases}$$
(29)

and all of the regions  $H^+$  and  $H^-$  are R- or  $\bar{R}$ -regions, as follows:

(a). For k even, we have

$$[H'_{\mathbf{l}}(a,b,k)^{+},H'_{\mathbf{l}}(a,b,k)^{-}] = \begin{cases} [\bar{R}_{\mathbf{l}-\mathbf{l},\emptyset}((a-1)/2),R_{\emptyset,\mathbf{l}}((a+k-1)/2)], & a \text{ odd, } l_{1} = 1, \\ [R_{\mathbf{l}-\mathbf{l},\emptyset}((a-1)/2),R_{\emptyset,\mathbf{l}}((a+k-1)/2)], & a \text{ odd, } l_{1} > 1, \\ [\bar{R}_{\mathbf{l},\emptyset}((a-2)/2),R_{\emptyset,\mathbf{l}^{(m)}}((a+k)/2)], & a \text{ even.} \end{cases}$$
(30)

(b). For k odd, we have

$$[H'_{\mathbf{l},\mathbf{q}}(a,b,k)^{+},H'_{\mathbf{l},\mathbf{q}}(a,b,k)^{-}] = \begin{cases} [R_{\mathbf{q},\mathbf{l}^{(m)}}((a-1)/2), \bar{R}_{\mathbf{l},\mathbf{q}}((a+k)/2)], & a \text{ odd,} \\ [R_{\mathbf{q},\mathbf{l}}((a-2)/2), \bar{R}_{\mathbf{l},\mathbf{q}^{(n)}}((a+k+1)/2)], & a \text{ even,} \end{cases}$$
(31)

and

$$[\bar{H}'_{\mathbf{l},\mathbf{q}}(a,b,k)^{+},\bar{H}'_{\mathbf{l},\mathbf{q}}(a,b,k)^{-}] = \begin{cases} [\bar{R}_{\mathbf{q},\mathbf{l}^{(m)}}((a-1)/2), R_{\mathbf{l},\mathbf{q}}((a+k)/2)], & a \text{ odd,} \\ [\bar{R}_{\mathbf{q},\mathbf{l}}((a-2)/2), R_{\mathbf{l},\mathbf{q}^{(n)}}((a+k+1)/2)], & a \text{ even.} \end{cases}$$
(32)

One may wonder why the prefactors in (29) have the particular fraction form indicated. Our proof will show that we can in fact rephrase the theorem in an alternate form as follows.

**Theorem 11.** Let H be one of the regions  $H'_{\mathbf{l}}(a,b,k)$ ,  $H'_{\mathbf{l},\mathbf{q}}(a,b,k)$  or  $\bar{H}'_{\mathbf{l},\mathbf{q}}(a,b,k)$ , and let  $\ell'$  be the axis with respect to which the holes in H are symmetric. Then we have<sup>22</sup>

$$M(H) = \begin{cases} \frac{a+b+k}{a+k} \cdot 2^{w_{\ell'}(H)} M(\widehat{H}^{+}) M(\widehat{H}^{-}), & a \text{ odd,} \\ \frac{a+b+k}{a+2b+2k} \cdot 2^{w_{\ell'}(H)} M(\widehat{H}^{+}) M(\widehat{H}^{-}), & a \text{ even,} \end{cases}$$
(33)

and all of the regions  $\widehat{H}^+_{\ell'}$  and  $\widehat{H}^-_{\ell'}$  are R- or  $\bar{R}$ -regions, as follows:

<sup>&</sup>lt;sup>21</sup>Here  $H^+$  and  $H^-$  are the "half-regions" obtained from the nearly symmetric hexagon with holes H by the procedure described before the statement of Theorem 2 (see the middle picture in Figure 25 for an example).

<sup>&</sup>lt;sup>22</sup>Here  $\widehat{H}^+$  and  $\widehat{H}^-$  are the "half-regions" obtained from the nearly symmetric hexagon with holes H by the procedure described before the statement of Theorem 2 (see the middle picture in Figure 26 for an example).

(a). For k even, we have

$$[\widehat{H'}_{\mathbf{l}}(a,b,k)^{+},\widehat{H'}_{\mathbf{l}}(a,b,k)^{-}] = \begin{cases} [R_{\emptyset,\mathbf{l}}((a+k-3)/2), \bar{R}_{\mathbf{l}-\mathbf{l},\emptyset}((a+1)/2)], & a \text{ odd, } l_{1} = 1, \\ [R_{\emptyset,\mathbf{l}}((a+k-3)/2), R_{\mathbf{l}-\mathbf{l},\emptyset}((a+1)/2)], & a \text{ odd, } l_{1} > 1, \\ [R_{\emptyset,\mathbf{l}^{(m)}}((a+k-2)/2), \bar{R}_{\mathbf{l},\emptyset}(a/2)], & a \text{ even.} \end{cases}$$
(34)

(b). For k odd, we have

$$[\widehat{H'}_{\mathbf{l},\mathbf{q}}(a,b,k)^{+},\widehat{H'}_{\mathbf{l},\mathbf{q}}(a,b,k)^{-}] = \begin{cases} [\bar{R}_{\mathbf{l},\mathbf{q}}((a+k-2)/2), R_{\mathbf{q},\mathbf{l}^{(m)}}((a+1)/2)], & a \text{ odd,} \\ [\bar{R}_{\mathbf{l},\mathbf{q}^{(n)}}((a+k-1)/2), R_{\mathbf{q},\mathbf{l}}(a/2)], & a \text{ even,} \end{cases}$$
(35)

and

$$[\widehat{\overline{H}'}_{\mathbf{l},\mathbf{q}}(a,b,k)^{+},\widehat{\overline{H}'}_{\mathbf{l},\mathbf{q}}(a,b,k)^{-}] = \begin{cases} [R_{\mathbf{l},\mathbf{q}}((a+k-2)/2), \bar{R}_{\mathbf{q},\mathbf{l}^{(m)}}((a+1)/2)], & a \text{ odd,} \\ [R_{\mathbf{l},\mathbf{q}^{(n)}}((a+k-1)/2), \bar{R}_{\mathbf{q},\mathbf{l}}(a/2)], & a \text{ even.} \end{cases}$$
(36)

Remark 3. The most striking part of Theorem 10 is that the number of lozenge tilings is almost as if given by the factorization theorem — although the factorization theorem does not apply, as the regions are not symmetric! More precisely, the number of lozenge tilings is obtained by multiplying the quantity on the right hand side of the factorization theorem (which makes sense, with the definition of the regions  $H^+$  and  $H^-$  given before the statement of Theorem 1) by one of the simple fractions  $\frac{a+b+k}{a+2b+k}$  or  $\frac{a+b+k}{a}$ , according as a is odd or even, respectively; a similar statement holds for Theorem 11. This phenomenon seems to be essentially dependent on the structure of our holes. Even for a very simple change in their definition (for instance, having just two oppositely oriented triangular holes of side two), numerical data strongly indicates that such a simple relationship does not hold anymore. This also invites one to find a more direct proof.

It turns out that equations (29) and (33) can be combined to obtained the following result, which expresses the number of tilings of the regions  $H'_{\mathbf{l},\mathbf{q}}(a,b,k)$ ,  $H'_{\mathbf{l},\mathbf{q}}(a,b,k)$  or  $\bar{H}'_{\mathbf{l},\mathbf{q}}(a,b,k)$  directly in terms of the number of tilings of two very closely related regions of the corresponding unprimed type.

**Theorem 12.** Consider one of the regions  $H'_{\mathbf{l}}(a,b,k)$ ,  $H'_{\mathbf{l},\mathbf{q}}(a,b,k)$  or  $\bar{H}'_{\mathbf{l},\mathbf{q}}(a,b,k)$ , and denote it for short by H'(a). Denote by H(a) the corresponding unprimed region of the same parameters (the number of lozenge tilings of H(a) is given by Theorem 9 and the formulas in Theorem 8). Then we have

$$M(H'(a)) = \begin{cases} \frac{a+b+k}{\sqrt{(a+k)(a+2b+k)}} \sqrt{M(H(a-1))M(H(a+1))}, & a \text{ odd,} \\ \frac{a+b+k}{\sqrt{a(a+2b+2k)}} \sqrt{M(H(a-1))M(H(a+1))}, & a \text{ even.} \end{cases}$$
(37)

Remark 4. The above result has the following pleasing geometrical interpretation. Suppose we place a two-sided mirror along the axis  $\ell'$  with respect to which the holes in H'(a) are symmetric. Consider the region seen in the mirror from its left (this is precisely H(a+1)), and also the region seen in the mirror from its right (which is precisely H(a-1)). Then, up to a simple factor which depends on the parity of a, M(H'(a)) is just the geometric mean of the numbers of tilings of these two regions.

Our proof of Theorems 10 and 11 consists of two ingredients: (1) the lemma below, which can be obtained directly from the definitions of the polynomials  $P_{\mathbf{l},\mathbf{q}}(x)$  and  $\bar{P}_{\mathbf{l},\mathbf{q}}(x)$ , and (2) Theorem 2.

**Lemma 13.** For lists of strictly increasing positive integers  $\mathbf{l}=(l_1,\ldots,l_m)$  and  $\mathbf{q}=(q_1,\ldots,q_n)$ , we have<sup>23</sup>

$$\frac{P_{\mathbf{l},\mathbf{q}}(x+1)}{P_{\mathbf{l},\mathbf{q}}(x)} = \frac{(2x+2l_m+2)!(2x+2l_m-2m+2n+3)!}{(2x+2l_m-m+n+2)!(2x+2l_m-m+n+3)!} \cdot \prod_{i=1}^{m} \left[ \frac{x+l_m+l_i-m+n+2}{x+l_m-l_i+1} \right] \prod_{i=1}^{n} \left[ \frac{x+l_m+q_i+1}{x+l_m-q_i-m+n+2} \right]$$
(38)

and

$$\frac{\bar{P}_{\mathbf{l},\mathbf{q}}(x+1)}{\bar{P}_{\mathbf{l},\mathbf{q}}(x)} = \frac{(2x+2l_m+1)!(2x+2l_m-2m+2n+2)!}{(2x+2l_m-m+n+1)!(2x+2l_m-m+n+2)!} \cdot \prod_{i=1}^{m} \left[ \frac{x+l_m+l_i-m+n+1}{x+l_m-l_i+1} \right] \prod_{i=1}^{n} \left[ \frac{x+l_m+q_i+1}{x+l_m-q_i-m+n+1} \right].$$
(39)

*Proof.* We present the proof for (38); the proof of (39) is completely analogous. From the

When m = 0 or n = 0, the same conventions apply as for equations (21) and (22).

definition of  $P_{\mathbf{l},\mathbf{q}}(x)$ ,

$$\frac{P_{l,q}(x+1)}{P_{l,q}(x)} = \frac{c_{l,q}B_{m,n}(x+l_m-m+1)}{c_{l,q}B_{m,n}(x+l_m-m)} \cdot \frac{\prod_{i=1}^{m} \prod_{j=i}^{l_i-1} (x+l_m-j+1)(x+l_m-m+n+j+3)}{\prod_{i=1}^{m} \prod_{j=i}^{l_i-1} (x+l_m-j)(x+l_m-m+n+j+2)} \\
\cdot \frac{\prod_{i=1}^{n} \prod_{j=i}^{q_i-1} (x+l_m-m+n-j+2)(x+l_m+j+2)}{\prod_{i=1}^{n} \prod_{j=i}^{q_i-1} (x+l_m-m+n-j+1)(x+l_m+j+1)} \\
= \frac{B_{m,n}(x+l_m-m+1)}{B_{m,n}(x+l_m-m)} \cdot \prod_{i=1}^{m} \left[ \frac{(x+l_m-i+1)(x+l_m-m+n+l_i+2)}{(x+l_m-l_i+1)(x+l_m-m+n+i+2)} \right] \\
\cdot \prod_{i=1}^{n} \left[ \frac{(x+l_m-m+n-i+2)(x+l_m+q_i+1)}{(x+l_m-q_i-m+n+2)(x+l_m+i+1)} \right] \\
= \frac{B_{m,n}(x+l_m-m+1)}{B_{m,n}(x+l_m-m)} \cdot \frac{(x+l_m-m+1)_m(x+l_m-m+2)_n}{(x+l_m-m+n+3)_m(x+l_m+2)_n} \\
\cdot \prod_{i=1}^{m} \left[ \frac{x+l_m+l_i-m+n+2}{x+l_m-l_i+1} \right] \prod_{i=1}^{n} \left[ \frac{x+l_m+q_i+1}{x+l_m-q_i-m+n+2} \right].$$

On the other hand, by the definition of  $B_{m,n}(x)$ ,

$$\frac{B_{m,n}(x+1)}{B_{m,n}(x)} = \frac{2^{-mn-m(m-1)/2}(x+n+2)_m(x+n+3)_m\langle x+3,x+n+1\rangle\langle x+\frac{5}{2},x+\frac{2n+3}{2}\rangle}{2^{-mn-m(m-1)/2}(x+n+1)_m(x+n+2)_m\langle x+2,x+n\rangle\langle x+\frac{3}{2},x+\frac{2n+1}{2}\rangle} 
\cdot \frac{\prod_{i=1}^n \frac{(x+i+1)_m}{(x+i+3/2)_m} \prod_{i=1}^m (2x+n+i+4)_{n+i-1}}{\prod_{i=1}^n \frac{(x+i)_m}{(x+i+1/2)_m} \prod_{i=1}^m (2x+n+i+2)_{n+i-1}} 
= \frac{(x+n+3)_m}{(x+n+1)_m} \cdot \frac{\langle x+3,x+n+1\rangle\langle x+\frac{5}{2},x+\frac{2n+3}{2}\rangle}{\langle x+2,x+n\rangle\langle x+\frac{3}{2},x+\frac{2n+1}{2}\rangle} 
\cdot \frac{(x+n+1)_m(x+3/2)_m}{(x+1)_m(x+n+3/2)_m} \cdot \frac{(2x+2n+3)_{2m}}{(2x+n+3)_m(2x+n+4)_m}.$$
(41)

Furthermore<sup>24</sup>,

$$\frac{\langle x+3, x+n+1\rangle\langle x+\frac{5}{2}, x+\frac{2n+3}{2}\rangle}{\langle x+2, x+n\rangle\langle x+\frac{3}{2}, x+\frac{2n+1}{2}\rangle} = \frac{\prod_{i=0}^{\lfloor \frac{n-2}{2}\rfloor} (x+3+i)_{n-1-2i} \prod_{i=0}^{\lfloor \frac{n-1}{2}\rfloor} (x+\frac{5}{2}+i)_{n-2i}}{\prod_{i=0}^{\lfloor \frac{n-2}{2}\rfloor} (x+2+i)_{n-1-2i} \prod_{i=0}^{\lfloor \frac{n-1}{2}\rfloor} (x+\frac{3}{2}+i)_{n-2i}} \\
= \prod_{i=0}^{\lfloor \frac{n-2}{2}\rfloor} \frac{x+n+1-i}{x+2+i} \prod_{i=0}^{\lfloor \frac{n-1}{2}\rfloor} \frac{x+n+\frac{3}{2}-i}{x+\frac{3}{2}+i} \\
= \frac{(2x+n+4)_n}{(2x+3)_n}.$$
(42)

Combining (40)–(42) and performing some algebraic manipulation, one obtains (38).

Proof of Theorems 10 and 11. Our proof is based on Theorem 2 and Lemma 13. The details of the arguments depend on the parities of k and a, as well as on whether  $l_1 = 1$  or  $l_1 > 1$ . We only present the proof in one of these cases, as the proofs of the remaining cases are very similar.

Suppose that k is even, a is odd, and  $l_1 = 1$ .

Apply the semi-factorization theorem (Theorem 2) to the region  $H = H'_1(a, b, k)$ . Note that in the case that we are assuming we have (1) m = b and (2)  $l_m = l_b = b + \frac{k}{2}$ . These equalities can be obtained by using the fact that the number of up-pointing and down-pointing unit triangles in the region are the same (a necessary condition for the existence of a tiling, as each lozenge covers one unit triangle of each type) or by expressing the same length in two different ways.

This application of Theorem 2 involves two different zigzag cuts (as described before the statement of Theorem 2) and produces four half-regions  $H^+$ ,  $H^+$ ,  $\hat{H}^+$  and  $\hat{H}^-$ . It is not hard to see that all these four belong to the two families defined in subsection 4.2. More precisely, we have

$$H^{+} = R_{\emptyset,\mathbf{l}}((a+k-1)/2),$$
  

$$H^{-} = \bar{R}_{\mathbf{l}-1,\emptyset}((a-1)/2),$$
  

$$\hat{H}^{+} = R_{\emptyset,\mathbf{l}}((a+k-3)/2),$$
  

$$\hat{H}^{-} = \bar{R}_{\mathbf{l}-1,\emptyset}((a+1)/2).$$

Thus, by Theorem 2,  $M(H) = M(H'_1(a, b, k))$  can be expressed as

$$2^{\mathbf{w}_{l'}(H)-1} \left( M(R_{\emptyset,\mathbf{l}}((a+k-1)/2)) M(\bar{R}_{\mathbf{l}-1,\emptyset}((a-1)/2)) + M(R_{\emptyset,\mathbf{l}}((a+k-3)/2)) M(\bar{R}_{\mathbf{l}-1,\emptyset}((a+1)/2)) \right).$$
(43)

 $<sup>2^{4}</sup>$ In the last equality, we use the fact that for any integer n,  $(\lfloor \frac{n-2}{2} \rfloor + 1) + (\lfloor \frac{n-1}{2} \rfloor + 1) = n$ .

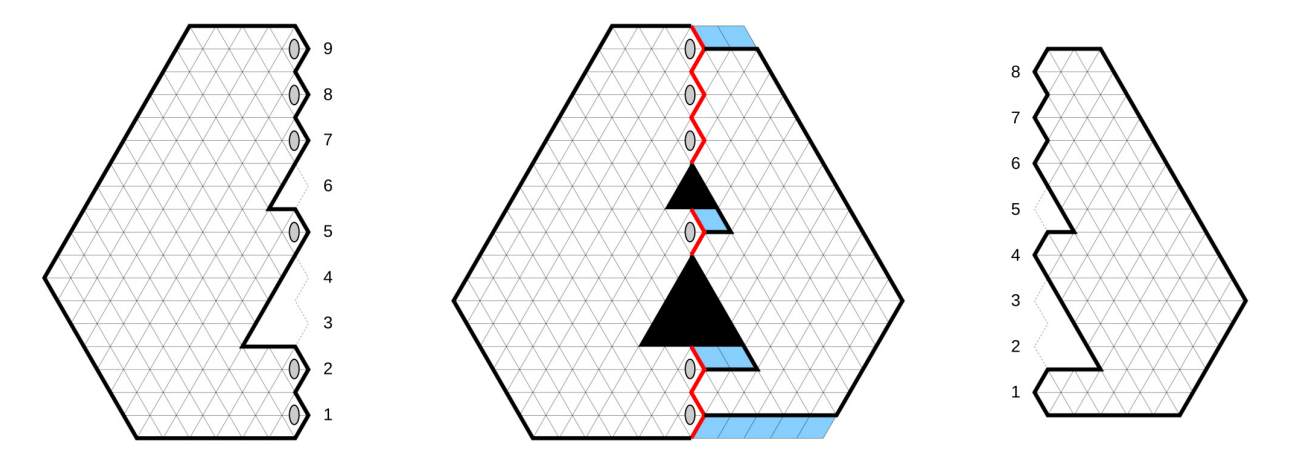


Figure 25: Decomposition of  $H = H'_{\mathbf{l}}(a,b,k)$  for  $a=5,\ b=6,\ k=6$  and  $\mathbf{l}=(1,2,5,7,8,9)$  into the half-regions  $H^+$  and  $H^-$  (see the notation in Theorem 2). The left half,  $H^+$ , is precisely our region  $R_{\emptyset,\mathbf{l}}((a+k-1)/2)$  (see subsection 4.2), while the one on the right,  $H^-$ , is congruent to our region  $\bar{R}_{\mathbf{l}-1,\emptyset}((a-1)/2)$ .

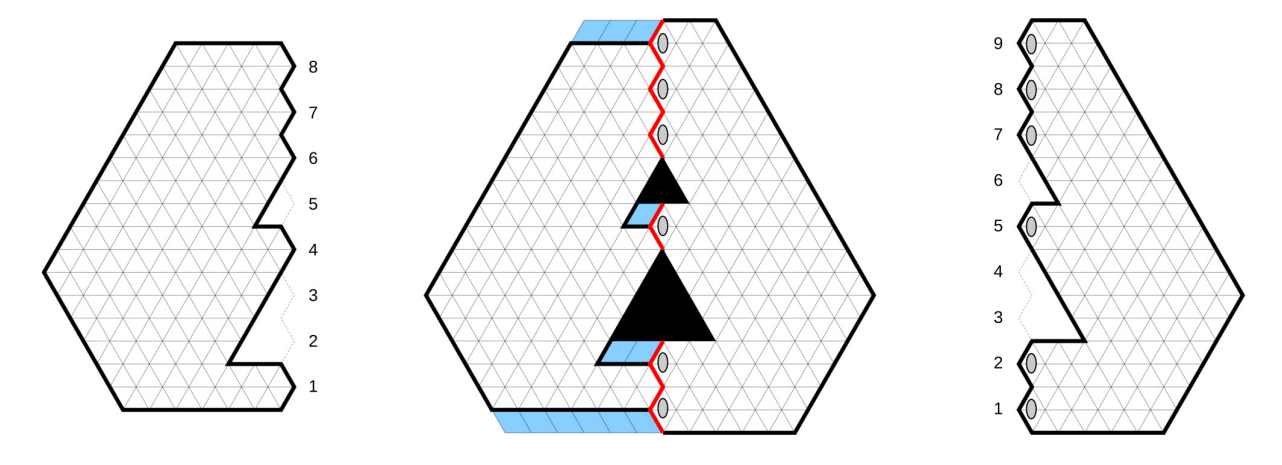


Figure 26: Decomposition of  $H'_{\mathbf{l}}(a,b,k)$  for  $a=5,\ b=6,\ k=6$  and  $\mathbf{l}=(1,2,5,7,8,9)$  into the half-regions  $\widehat{H}^+$  (the left half-region in the center picture) and  $\widehat{H}^-$  (the right half-region). We have  $\widehat{H}^+ = \overline{R}_{\mathbf{l}-1,\emptyset}((a+1)/2)$ , while  $\widehat{H}^-$  is the reflection across the vertical of  $R_{\emptyset,\mathbf{l}}((a+k-3)/2)$ .

On the other hand, by Lemma 13, we have

$$\frac{M(R_{\emptyset,\mathbf{l}}((a+k-1)/2))}{M(R_{\emptyset,\mathbf{l}}((a+k-3)/2))} = \frac{P_{\emptyset,\mathbf{l}}((a+k-1)/2)}{P_{\emptyset,\mathbf{l}}((a+k-3)/2)}$$

$$= \frac{(a+k-1)!(a+2b+k)!}{(a+b+k-1)!(a+b+k)!} \cdot \prod_{i=1}^{b} \left[ \frac{(a+k-3)/2+l_i+1}{(a+k-3)/2-l_i+b+2} \right]$$

$$= \frac{(a+k-1)!(a+2b+k)!}{(a+b+k-1)!(a+b+k)!} \cdot \prod_{i=1}^{b} \left[ \frac{a+k+2l_i-1}{a+2b+k-2l_i+1} \right]$$
(44)

and

$$\frac{M(\bar{R}_{l-1,\emptyset}((a+1)/2))}{M(\bar{R}_{l-1,\emptyset}((a-1)/2)))} = \frac{\bar{P}_{l-1,\emptyset}((a+1)/2)}{\bar{P}_{l-1,\emptyset}((a-1)/2))}$$

$$= \frac{(a+2l_b-2)!(a+2l_b-2b+1)!}{(a+2l_b-b-1)!(a+2l_b-b)!} \prod_{i=1}^{b-1} \left[ \frac{(a-1)/2+l_b+l_{i+1}-b}{(a-1)/2+l_b-l_{i+1}+1} \right]$$

$$= \frac{(a+2l_b-2)!(a+2l_b-2b+1)!}{(a+2l_b-b-1)!(a+2l_b-b)!} \prod_{i=1}^{b-1} \left[ \frac{a+2l_b+2l_{i+1}-2b-1}{a+2l_b-2l_{i+1}+1} \right]$$

$$= \frac{(a+2b+k-2)!(a+k+1)!}{(a+b+k-1)!(a+b+k)!} \prod_{i=1}^{b-1} \left[ \frac{a+k+2l_{i+1}-1}{a+2b+k-2l_{i+1}+1} \right]$$
(45)

Therefore, if we use the two equalities above and the fact that  $l_1 = 1$ , we obtain

$$\frac{M(R_{\emptyset,\mathbf{l}}((a+k-1)/2)) M(\bar{R}_{\mathbf{l}-1,\emptyset}((a-1)/2))}{M(R_{\emptyset,\mathbf{l}}((a+k-3)/2)) M(\bar{R}_{\mathbf{l}-1,\emptyset}((a+1)/2))}$$

$$= \frac{(a+k-1)!}{(a+k+1)!} \cdot \frac{(a+2b+k)!}{(a+2b+k-2)!} \cdot \frac{a+k+1}{a+2b+k-1}$$

$$= \frac{a+2b+k}{a+k}.$$
(46)

This implies that, if we factor out  $M(R_{\emptyset,l}((a+k-3)/2)) M(\bar{R}_{l-1,\emptyset}((a+1)/2))$  from (43), we obtain

$$M(H) = M(H'_{\mathbf{l}}(a,b,k))$$

$$= 2^{w_{l'}(H)-1} \left[ \frac{a+2b+k}{a+k} + 1 \right] M(R_{\emptyset,\mathbf{l}}((a+k-3)/2)) M(\bar{R}_{\mathbf{l}-1,\emptyset}((a+1)/2))$$

$$= \frac{2a+2b+2k}{a+k} \cdot 2^{w_{l'}(H)-1} M(R_{\emptyset,\mathbf{l}}((a+k-3)/2)) M(\bar{R}_{\mathbf{l}-1,\emptyset}((a+1)/2))$$

$$= \frac{a+b+k}{a+k} \cdot 2^{w_{l'}(H)} M(R_{\emptyset,\mathbf{l}}((a+k-3)/2)) M(\bar{R}_{\mathbf{l}-1,\emptyset}((a+1)/2)).$$
(47)

On the other hand, if we factor out  $M(R_{\emptyset,l}((a+k-1)/2)) M(\bar{R}_{l-1,\emptyset}((a-1)/2))$  from (43), we get

$$M(H) = M(H'_{\mathbf{1}}(a,b,k))$$

$$= 2^{w_{l'}(H)-1} \left[ \frac{a+k}{a+2b+k} + 1 \right] M(R_{\emptyset,\mathbf{I}}((a+k-1)/2)) M(\bar{R}_{\mathbf{I}-\mathbf{I},\emptyset}((a-1)/2))$$

$$= \frac{2a+2b+2k}{a+2b+k} \cdot 2^{w_{l'}(H)-1} M(R_{\emptyset,\mathbf{I}}((a+k-1)/2)) M(\bar{R}_{\mathbf{I}-\mathbf{I},\emptyset}((a-1)/2))$$

$$= \frac{a+b+k}{a+2b+k} \cdot 2^{w_{l'}(H)} M(R_{\emptyset,\mathbf{I}}((a+k-1)/2)) M(\bar{R}_{\mathbf{I}-\mathbf{I},\emptyset}((a-1)/2)).$$
(48)

This completes the proof in the case when k even, a odd, and  $l_1 = 1$ . The proof of the remaining cases works in exactly the same manner: we apply Theorem 2 to M(H), use Lemma 13, and finally use some identities that the indices satisfy (which we can obtain by using the fact that the region consists of the same number of up- and down-pointing unit triangles or by expressing the same length in two different ways; for example, when k even, a odd, and  $l_1 = 1$ , we have m = b and  $l_m = l_b = b + \frac{k}{2}$ ).

Proof of Theorem 12. Let H be one of the regions  $H'_{\mathbf{l}}(a,b,k)$ ,  $H'_{\mathbf{l},\mathbf{q}}(a,b,k)$  or  $\bar{H}'_{\mathbf{l},\mathbf{q}}(a,b,k)$ . Note that  $H^+$  and  $\widehat{H}^-$  are the same R or  $\bar{R}$  region, just the x-argument in the former is one more that in the latter. The same holds for  $\widehat{H}^+$  and  $H^-$ . This guarantees that  $\widehat{H}^+$  fits to the right of  $H^+$  to allow a reverse application of the factorization theorem, and  $H^-$  fits to the left of  $\widehat{H}^-$  to do the same. The proof follows then by multiplying together equations (29) and (33), pairing together the factors  $M(H^+)$  and  $M(\widehat{H}^+)$ , pairing also  $M(H^-)$  and  $M(\widehat{H}^-)$ , and applying the factorization theorem in reverse twice.

## 5 Nearly symmetric hexagons with a shamrock or fern hole

An *S-cored hexagon* is a hexagon from which a *shamrock* — the union of an up-pointing triangular core and three down-pointing triangular lobes touching the core at its three vertices — is removed (see [9]). Simple product formulas for the number of lozenge tilings of a symmetric *S*-cored hexagon were given in [7] and [25].

In this section we solve another open problem of Lai (namely, [24, Problem 27]), which asks to find and prove a simple product formula for the number of lozenge tilings of the region obtained from a symmetric S-cored hexagon by translating the shamrock hole one unit southeast; we call such a region a nearly symmetric S-cored hexagon (see Theorem 14). In addition, we prove a similar formula for F-cored hexagons — regions obtained from hexagons by removing a  $fern^{25}$  — the union of contiguous triangular lobes of alternating orientation lined up along a horizontal lattice line — instead of a shamrock (such a region will be called a nearly symmetric F-cored hexagon; see Theorem 16).

<sup>&</sup>lt;sup>25</sup>Ferns were introduced in [6], where a simple product formula was proved for the number of tilings of a hexagon with a fern removed from its center. The number of tilings of an *F*-cored hexagon which is symmetric about a vertical axis was determined in [23].

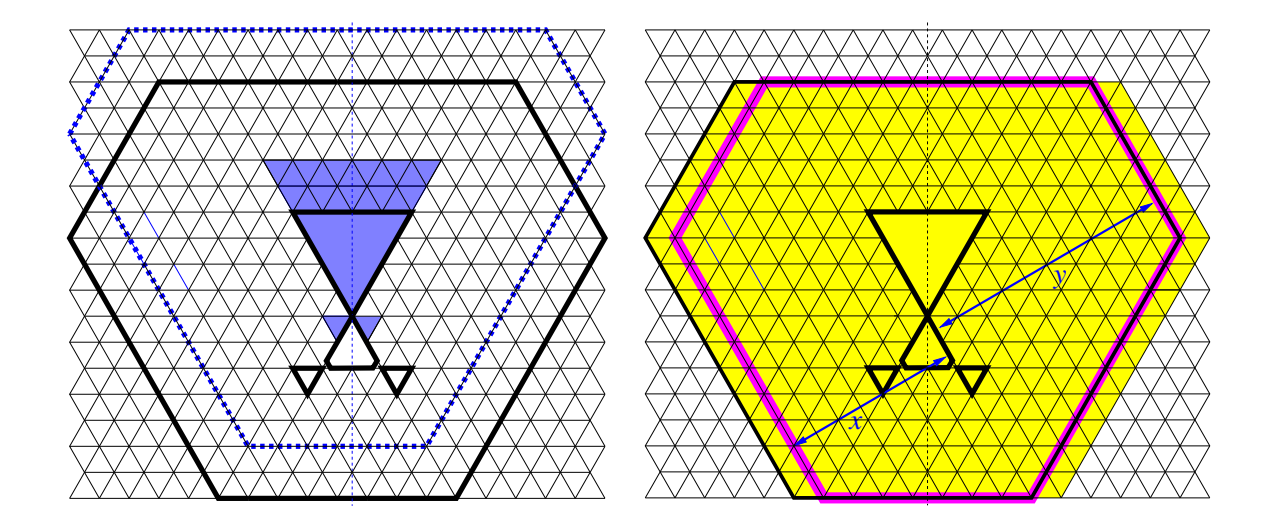


Figure 27: Left. Squeezing out the central lobe of the shamrock in a nearly symmetric S-cored hexagon; the original region is shown in black, while the region obtained from it after the squeezing is indicated in blue. Right. The distances x and y between a support line and the opposite sides of the outer hexagon in the thin symmetrization  $H_1$  (shown inside the magenta contour) of H'; the thick symmetrization  $H_2$  is shaded in yellow.

**Theorem 14.** Let H' be a nearly symmetric S-cored hexagon in which the side-lengths of the triangular lobes are  $\alpha$  for the top one,  $\beta$  for the two bottom ones, and  $\mu$  for the central one; let the side-lengths of the outer hexagon be  $x + \alpha + 2\beta$ ,  $y + \mu$ ,  $y + \alpha + 2\beta$ ,  $x + \mu$ ,  $y + \alpha + 2\beta$ ,  $y + \mu$  (clockwise from top; see the picture on the left in Figure 27 for an example). Let  $\ell'$  be the vertical symmetry axis of the removed shamrock.

Denote by  $H_1$  the region consisting of the union of the portion of H' to the right of  $\ell'$  with its reflection across  $\ell'$  (i.e., the region seen if  $\ell'$  was a mirror and one looks in it from the right; see the picture on the right in Figure 27 for an illustration); let  $H_2$  be the analogous region determined by the portion of H' to the left of  $\ell'$ . Then we have

$$M(H')^2 = f M(H_1) M(H_2),$$
 (49)

where

$$f = \begin{cases} \frac{(x+y+\alpha+2\beta+\mu)^2}{(x+\alpha+2\beta+\mu)(x+2y+\alpha+2\beta+\mu)}, & x \text{ odd,} \\ \frac{(x+y+\alpha+2\beta+\mu)^2}{x(x+2y+2\alpha+4\beta+2\mu)}, & x \text{ even.} \end{cases}$$
(50)

With the formulas for the number of lozenge tilings of  $H_1$  and  $H_2$  — which are, by construction, symmetric S-cored hexagons — given in [7] and [25], this provides an explicit product formula for M(H'), and thus solves Lai's Problem 27 in the list of open problems [24].

*Proof.* We recall the "bowtie squeezing theorem" [10, Theorem 1]. A triad hexagon is a region obtained from a hexagon by removing three bowtie-shaped holes positioned as

illustrated in [10, Figure 1]. Bowtie squeezing is an operation that turns a triad hexagon into another triad hexagon by squeezing part (or all) of a lobe of a bowtie into the other lobe; the position of the node of the squeezed bowtie as well as the shape of the other two bowties remain the same, but the relative position of the bowties and the boundary hexagon change (an illustrative example is shown [10, Figure 1] — see that paper for the details; the picture on the left in Figure 27 shows a special case). Then [10, Theorem 1] states that if the region Q is obtained from the triad hexagon R by a sequence of bowtie squeezing operations, then we have<sup>26</sup>

$$\frac{M(R)}{M(Q)} = \frac{w^{(R)} \frac{k_A^{(R)} k_B^{(R)} k_C^{(R)}}{k_{BC}^{(R)} k_{AC}^{(R)} k_{AB}^{(R)}}}{w^{(Q)} \frac{k_{A_1}^{(Q)} k_{B_1}^{(Q)} k_{C_1}^{(Q)}}{k_{B_1C_1}^{(Q)} k_{A_1C_1}^{(Q)} k_{A_1B_1}^{(Q)}},$$
(51)

where the weight  $\mathbf{w}^{(R)}$  depends only on the shapes of the three bowties and their relative positions (the precise expression is given in [10, (2.2)], but we don't need it here), and the point couples like  $\mathbf{k}_A^{(R)}$  (resp., the line couples like  $\mathbf{k}_{BC}^{(R)}$ ) have the following common definition: if  $\mathbf{h}(n)$  is the hyperfactorial  $\mathbf{h}(n) = 0! \, 1! \, \cdots \, (n-1)!$ , the point couple  $\mathbf{k}_A^{(R)}$  is defined to be  $\mathbf{h}(u) \, \mathbf{h}(d)$ , where u and d are the distances from A to the pair of opposite sides of the outer hexagon towards which the 60° degree double cone at A contained in the bowtie points (for line couples, u and d are the distances from the line to the sides of the hexagon parallel to it).

Consider our nearly symmetric S-cored hexagon H' (indicated in black in Figure 27). Its shamrock-shaped hole can be regarded as a triad of bowties: the top bowtie has upper lobe of side  $\alpha$  and lower lobe of side  $\mu$ , while the other two bowties consist of just their lower lobes, both of side  $\beta$ . Let T' be the region obtained from H' by completely squeezing out the bottom lobe of the top bowtie (T' is indicated in blue in Figure 27). Applying equation (51) for R = H' and Q = T' we get

$$\frac{M(H')}{M(T')} = \frac{\frac{W^{(H')}}{k_{AC}^{(H')}} \frac{k_{A}^{(H')}}{k_{BC}^{(H')}} \frac{k_{C}^{(H')}}{k_{AC}^{(H')}} k_{AB}^{(H')}}{\frac{k_{AC}^{(T')}}{k_{AC}^{(T')}} \frac{k_{AC}^{(T')}}{k_{AB}^{(T')}} \frac{k_{AB}^{(H')}}{k_{AC}^{(T')}} = \frac{W^{(H')}}{k_{AC}^{(H')}} \frac{k_{A}^{(H')}}{k_{AC}^{(H')}} \frac{k_{AB}^{(H')}}{k_{AB}^{(T')}},$$
(52)

where at the last equality we used that  $\mathbf{k}_B^{(H')} = \mathbf{k}_{B_1}^{(T')}$ ,  $\mathbf{k}_C^{(H')} = \mathbf{k}_{C_1}^{(T')}$  and  $\mathbf{k}_{BC}^{(H')} = \mathbf{k}_{B_1C_1}^{(T')}$  (these equalities hold because the pairs of distances involved in the couples claimed to be equal are identical).

Consider now the "thin symmetrization"  $H_1$  described in the statement of the theorem, and let  $T_1$  be the region obtained from it by completely squeezing out the bottom lobe of

<sup>&</sup>lt;sup>26</sup>Here A, B and C (resp.,  $A_1$ ,  $B_1$  and  $C_1$ ) are the nodes — i.e., the points where the two lobes meet — of the bowties in the triad hexagon R (resp., Q), counterclockwise from top.

the top bowtie. Equation (51) then similarly gives

$$\frac{M(H_1)}{M(T_1)} = \frac{w^{(H_1)} \frac{k_A^{(H_1)}}{k_{AC}^{(H_1)} k_{AB}^{(H_1)}}}{w^{(T_1)} \frac{k_{A_1}^{(T_1)}}{k_{A_1}^{(T_1)} k_{A_1B_1}^{(T_1)}}}.$$
(53)

Note that the point couples  $k_A^{(H')}$  are  $k_A^{(H_1)}$  equal, since the distances involved in them are identical; similarly,  $k_{A_1}^{(T')} = k_{A_1}^{(T_1)}$ . Furthermore, we have  $w^{(H')} = w^{(H_1)}$ , because  $w^{(R)}$  depends only on the shapes and relative positions of the bowties in the triad hexagon; similarly,  $w^{(T')} = w^{(T_1)}$ . Therefore, combining (52) and (53) we obtain

$$\frac{M(H')/M(H_1)}{M(T')/M(T_1)} = \frac{k_{AC}^{(H_1)} k_{AB}^{(H_1)}}{k_{AC}^{(H')} k_{AB}^{(H')}} \frac{k_{A_1C_1}^{(T')} k_{A_1B_1}^{(T')}}{k_{A_1C_1}^{(T_1)} k_{A_1B_1}^{(T_1)}}.$$
(54)

Repeating the argument with  $H_1$  replaced by the thick symmetrization  $H_2$  of H' yields

$$\frac{M(H')/M(H_2)}{M(T')/M(T_2)} = \frac{k_{AC}^{(H_2)} k_{AB}^{(H_2)}}{k_{AC}^{(H')} k_{AB}^{(H')}} \frac{k_{A_1C_1}^{(T')} k_{A_1B_1}^{(T')}}{k_{A_1C_1}^{(T_2)} k_{A_1B_1}^{(T_2)}}.$$
(55)

Multiply the last two equations side by side to obtain

$$\frac{M(H')^{2}/(M(H_{1})M(H_{2}))}{M(T')^{2}/(M(T_{1})M(T_{2}))} = \frac{k_{AC}^{(H_{1})}k_{AB}^{(H_{1})}k_{AB}^{(H_{1})}k_{A_{1}C_{1}}^{(T')}k_{A_{1}B_{1}}^{(T')}}{k_{AC}^{(H')}k_{AB}^{(H')}k_{A_{1}B_{1}}^{(T_{1})}k_{A_{1}B_{1}}^{(T)}} \frac{k_{AC}^{(H_{2})}k_{AB}^{(H_{2})}k_{AB}^{(H_{2})}k_{A_{1}B_{1}}^{(T')}$$

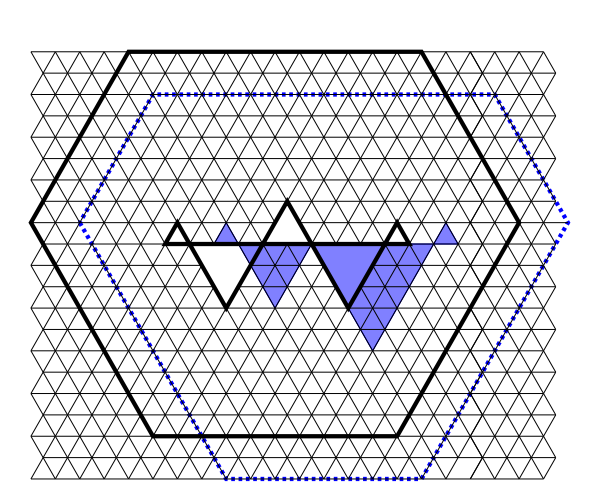
Denoting by x and y the distances from the line supporting the top and right lobes in  $H_1$  to the northeast and southwest sides of the boundary (see the picture on the right in Figure 27), the factors involving H-regions on the right hand side above combine to

$$\frac{h(x) h(y)}{h(x+1) h(y)} \frac{h(x) h(y)}{h(x) h(y+1)} \frac{h(x+1) h(y+1)}{h(x+1) h(y)} \frac{h(x+1) h(y+1)}{h(x) h(y+1)} = 1.$$
 (57)

The same calculation shows that the factors involving T-regions combine to 1 as well. Therefore, the entire right hand side of (56) is 1, and we get

$$\frac{M(H')^2}{M(H_1) M(H_2)} = \frac{M(T')^2}{M(T_1) M(T_2)}.$$
 (58)

Since Theorem 12 applies to T' (indeed, due to forced lozenges, the removal of the three down-pointing lobes that meet at a point is equivalent, from the point of view of counting lozenge tilings, with the removal of a single down-pointing triangle of side  $\alpha + 2\beta + \mu$ ), the statement follows from (58) by noticing that the a-, b- and k-values of the parameters in Theorem 12 corresponding to T' are x, y and  $\alpha + 2\beta + \mu$ , respectively.



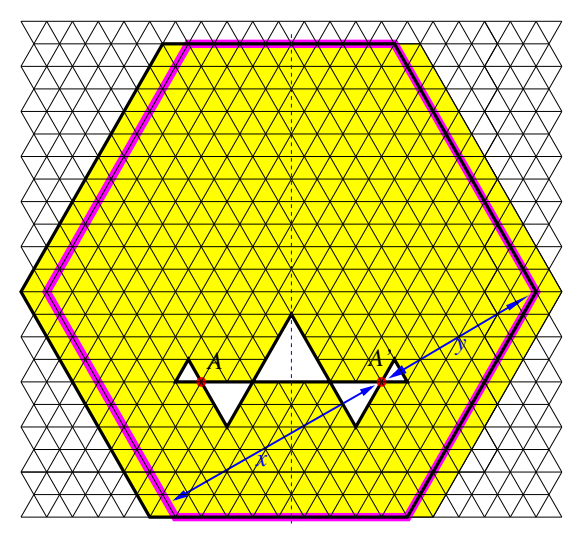


Figure 28: Left. Squeezing out the central lobe of a nearly symmetric F-cored hexagon. Right. The distances x and y between the node A' and the opposite sides of the outer hexagon in the thin symmetrization  $H_1$  (inside the magenta contour) of H'; the yellow shading indicates  $H_2$ .

The operation of lobe squeezing can also be defined for a hexagon from which a collection of disjoint collinear ferns has been removed. The definition is analogous to the bowtie squeezing operation (which really squeezes one lobe of a given bowtie into the other) described in [10].

For simplicity, suppose that only one fern has been removed from the hexagon. The picture on the left in Figure 28 illustrates such an example: the black solid lines show the original region, while shown in blue is the region that results by completely squeezing the central lobe into the one to its right. In general, let R be a hexagon with a fern removed, and let A be a node of the fern (i.e., a point where two lobes meet). Then the region obtained from R by squeezing the lobe to the left of A into the lobe to the right of A by d units is the region Q described by: (1) Q is a hexagon with a fern removed (2) the boundary hexagon of Q is obtained from that of R by pushing in three of its sides by d units, and pushing out the other three by d units (which three are pushed in and which are pushed out is determined by the direction of the squeezing, which pulls in the three sides in the back and pushes out the three sides in the front), and (3) the removed fern of Q is obtained from that of R by keeping the node A fixed, shrinking the lobe to its left by d units (while "dragging along" the portion of the fern to the left of it), and inflating the lobe to the right of A by d units (while "pushing away" the portion of the fern to the right of this lobe).

The definition works in the same way for the case when a collection of ferns lined up along a common horizontal line has been removed from the hexagon — the only change is that in (3) above when we shrink and correspondingly inflate the two lobes at A, we translate to the right by d units the entire remaining portion of the system of ferns.

Consider a region R obtained from a hexagon by removing a collection of collinear

ferns. A node of R is a point A on one of the removed ferns where two lobes meet. A support line of R is a lattice line L that contains an edge of at least two lobes (with the exception of the common axis of the ferns, all support lines support precisely two lobes). The point couples  $k_A^{(R)}$  and line couples  $k_L^{(R)}$  are defined exactly like in [10] (these were also recalled at the beginning of the proof of Theorem 14). To define the weight  $w^{(R)}$ , label the unit lattice segments inside R which are on the common axis of the removed ferns by  $1, 2, 3, \ldots$ , from left to right. If I is the set of labels corresponding to the bases of the down-pointing lobes of the ferns, and I consists of the labels on the bases of the up-pointing lobes, then the weight  $w^{(R)}$  is defined to be

$$\mathbf{w}^{(R)} = \Delta(I)\Delta(J),\tag{59}$$

where for a set  $I = \{s_1, \ldots, s_k\}$  with elements listed in increasing order we define

$$\Delta(I) := \prod_{1 \le i < j \le k} (s_j - s_i). \tag{60}$$

We have the following analog of the bowtie squeezing theorem.

**Theorem 15.** Let R be a hexagonal region from which a system of co-axial ferns has been removed. Let Q be a region obtained from R by a sequence of lobe squeezings. Then we have

$$\frac{\mathcal{M}(R)}{\mathcal{M}(Q)} = \frac{\prod_{A \text{ node of } R} k_A^{(R)}}{\prod_{L \text{ support line of } R} k_L^{(R)}} \frac{\prod_{A \text{ node of } Q} k_A^{(R)}}{\prod_{L \text{ support line of } Q} k_L^{(Q)}}.$$
(61)

*Proof.* We can assume without loss of generality that Q is obtained from R by a single operation of lobe squeezing.

Let  $\overline{R}$  be the region obtained from R by the following procedure. Denote by  $R_1$  the region obtained by starting with the outer hexagon H of R, but removing from it, instead of the system of ferns, just those unit triangles contained in the system of ferns whose bases rest on their common axis l. Note that, due to forced lozenges, the region  $R_1$  has the same number of lozenge tilings as R. Next, construct a vertically symmetric hexagon  $\overline{H}$  so that l is its horizontal diagonal, and four of its sides — including the top and bottom ones — are one the same lattice lines as the corresponding sides of H. Finally, remove from  $\overline{H}$  the unit triangles that were removed to construct  $R_1$ , and in addition also runs of unit triangles along the portions of l outside H, chosen so as to force a unique tiling of the remaining portion of  $\overline{H} \setminus H$ ; the resulting region is what we define to be  $\overline{R}$ . Then we have  $M(\overline{R}) = M(R_1) = M(R)$ , and  $\overline{R}$  is precisely the kind of region to which the shuffling theorem of [26] applies.

This theorem concerns pairs of regions S and T which can be described as follows. The region S is a vertically symmetric hexagon with a set of unit triangles (both uppointing and down-pointing being allowed) removed from along its horizontal diagonal l.

The region T is obtained from S by "flipping" an arbitrary subset of the removed unit triangles, i.e. moving them to the position of their mirror image across l, and changing the boundary of the outer hexagon appropriately (the latter is needed in order to end up with a region with the same number of up- and down-pointing unit triangles, a necessary condition for the existence of lozenge tilings). Then the theorem states that M(S)/M(T) has a simple expression in terms of  $\Delta$  functions (60) of sets which record the positions of the removed unit triangles.

Let A be a node of the system of ferns in the given region R, and assume that Q was obtained from R by squeezing out d units of the lobe left of A into the lobe right of A. Consider the region  $\overline{R}$  defined above, and also the region  $\overline{Q}$  obtained by applying the same procedure to Q. Apply the shuffling theorem to the region  $\overline{R}$ , by flipping the run of d contiguous unit triangles just to the left of A. It is not hard to verify that the resulting region is precisely  $\overline{Q}$ .

Therefore, the shuffling theorem of [26] applies to the regions  $\overline{R}$  and  $\overline{Q}$ , and gives

$$\frac{\mathcal{M}(\overline{R})}{\mathcal{M}(\overline{Q})} = \frac{1/k_l^{(\overline{R})}}{1/k_l^{(\overline{Q})}} \frac{\Delta(X)\Delta(Y)}{\Delta(X')\Delta(Y')},\tag{62}$$

where X (resp., Y) is the set of labels<sup>27</sup> of the up-pointing (resp., down-pointing) unit triangles with bases on L which are removed from the outer hexagon of  $\overline{R}$ , while X' and Y' are the corresponding sets of labels for  $\overline{Q}$ .

After a straightforward (if lengthy) rearranging of the factors on the right hand side of (62), one can bring the expression on the right hand side of (62) to the form shown on the right hand side of (61). Since  $\frac{M(R)}{M(Q)} = \frac{M(\overline{R})}{M(\overline{Q})}$ , this completes the proof.

Remark 6. As pointed out in [6], it seems that shamrocks and ferns are the only shapes of holes that lead to simple product formulas when considering the number of lozenge tilings of a hexagon with a hole removed from its center. The above theorem and the statement (51) of [10, Theorem 1] take the common features of these shapes one step further, by providing a pleasingly unified form for the quantities that govern the number of lozenge tilings in regions related by lobe squeezing operations — up to the weights  $\mathbf{w}^{(R)}$  and  $\mathbf{w}^{(Q)}$ , the right hand side of (51) is precisely the same expression as that of (61)!

As an application of Theorem 15, we show that nearly symmetric hexagons with a fernshaped hole are related to their symmetric counterparts by essentially the same identity as in Theorems 12 and 14.

**Theorem 16.** Let H' be a nearly symmetric F-cored hexagon in which the side-lengths of the triangular lobes of the removed ferns are  $\alpha_1, \alpha_2, \cdots$  for the down-pointing ones, and  $\beta_1, \beta_2, \cdots$  for the up-pointing ones. Set  $\alpha = \alpha_1 + \alpha_2 + \cdots$  and  $\beta = \beta_1 + \beta_2 + \cdots$ , and let the side-lengths of the outer hexagon be  $x + \alpha$ ,  $y + \beta$ ,  $y + \alpha$ ,  $x + \beta$ ,  $y + \alpha$ ,  $y + \beta$  (clockwise from top). Let  $\ell'$  be the vertical symmetry axis of the removed fern.

<sup>&</sup>lt;sup>27</sup>The unit segments on l inside  $\overline{R}$  are labeled 1, 2, 3, ... from left to right.

Let the thin and thick symmetrizations of H',  $H_1$  and  $H_2$ , be defined as in the statement of Theorem 14. Then we have

$$M(H')^2 = f M(H_1) M(H_2),$$
 (63)

where

$$f = \begin{cases} \frac{(x+y+\alpha+\beta)^2}{(x+\alpha+\beta)(x+2y+\alpha+\beta)}, & x \text{ odd,} \\ \frac{(x+y+\alpha+\beta)^2}{x(x+2y+2\alpha+2\beta)}, & x \text{ even.} \end{cases}$$
(64)

*Proof.* The same approach as in the proof of Theorem 14 works. Let T' be the region obtained from H' by completely squeezing out the up-pointing lobes of the fern into the down-pointing lobes. Let  $T_1$  and  $T_2$  be the regions obtained in an analogous fashion from the symmetrized regions  $H_1$  and  $H_2$ .

Write down equation (61) for the pairs of regions (H', T') and  $(H_1, T_1)$ , and divide the resulting equations side by side to get an expression for  $\frac{M(H')/M(T')}{M(H_1)/M(T_1)}$ . Do the same for the pairs of regions (H', T') and  $(H_2, T_2)$  to get an expression for  $\frac{M(H')/M(T')}{M(H_2)/M(T_2)}$ . Finally, multiply these two equations to get an expression for  $\frac{M(H')^2/(M(H_1)M(H_2))}{M(T')^2/(M(T_1)M(T_2))}$ ; this will involve only point couples and line couples, as the weights w cancel out (since they are the same for H',  $H_1$  and  $H_2$ , and also for T',  $T_1$  and  $T_2$ ). If the distances x and y are as indicated in the picture on the right in Figure 28, the node couples pertaining to the regions H',  $H_1$  and  $H_2$  contribute

$$\prod_{A} \frac{k_{A}^{(H')} k_{A'}^{(H')}}{k_{A}^{(H_1)} k_{A'}^{(H_1)}} \frac{k_{A}^{(H')} k_{A'}^{(H')}}{k_{A}^{(H_2)} k_{A'}^{(H_2)}} \\
= \prod_{A} \frac{h(y+1) h(x) h(x+1) h(y)}{h(y) h(x) h(y) h(x)} \frac{h(y+1) h(x) h(x+1) h(y)}{h(y+1) h(x+1) h(y+1) h(x+1)} \\
= 1,$$
(65)

where the products are over the nodes of the fern to the left of its symmetry axis, and A' is the mirror image of A across this axis.

A similar calculation shows that the line couples pertaining to the regions H',  $H_1$  and  $H_2$  also contribute 1. The same calculations show that the factors pertaining to the regions T',  $T_1$  and  $T_2$  have an overall contribution of 1 as well. This shows that we have  $M(H')^2/(M(H_1)M(H_2)) = M(T')^2/(M(T_1)M(T_2))$ . The statement follows now from Theorem 12, upon observing that for the outer hexagon of T', the a-, b- and k-parameters in that theorem are x, y and  $\alpha + \beta$ , respectively.

## 6 Nearly symmetric hexagons with a lozenge hole

Using Theorem 2, we can also obtain a counterpart of a result of Fulmek and Krattenthaler which was presented in [17]. In [17] and [18], these authors considered the problem of

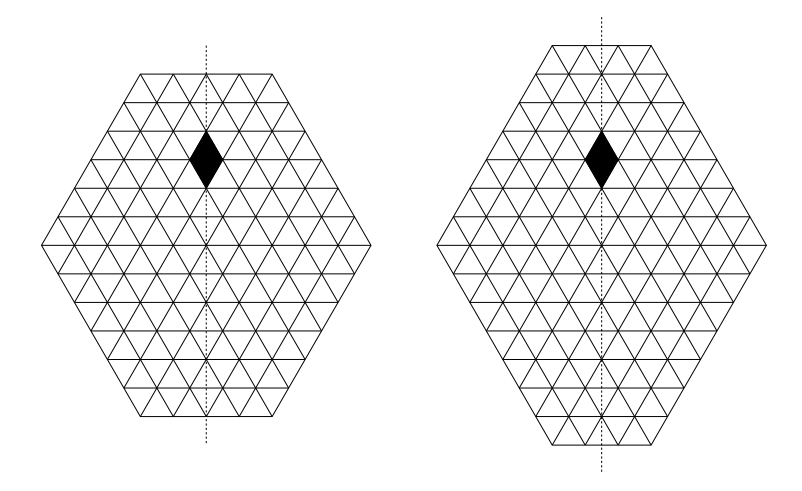


Figure 29: The regions considered in Theorem 17 (left) and Theorem 18 (right). These show the case when m = 2, N = 6, and l = 2.

enumerating lozenge tilings of a hexagon that has both vertical and horizontal symmetry—in this section, we will call this a *symmetric hexagon*<sup>28</sup>—which contain a fixed lozenge (or equivalently, tilings of a hexagon with a lozenge-shaped hole). In [17], they considered a symmetric hexagon, fixed a unit lozenge on the vertical<sup>29</sup> symmetry axis in an arbitrary position, and proved the following two results (Figure 29 illustrates the two types of regions considered).

**Theorem 17** (Theorem 1 in [17]). Let m be a non-negative integer and N a positive integer. The number of lozenge tilings of a hexagon with sides N, 2m, N, N, 2m, N, which contain the l-th lozenge on the symmetry axis which cuts through the sides of length 2m, equals<sup>30</sup>

$$\frac{m\binom{m+N}{m}\binom{m+N-1}{m}}{\binom{2m+2N-1}{2m}} \left( \sum_{e=0}^{l-1} (-1)^e \binom{N}{e} \frac{(N-2e)(\frac{1}{2})_e}{(m+e)(m+N-e)(\frac{1}{2}-N)_e} \right) \cdot \prod_{i=1}^{N} \prod_{j=1}^{N} \prod_{k=1}^{2m} \frac{i+j+k-1}{i+j+k-2}.$$
(66)

**Theorem 18** (Theorem 2 in [17]). Let m and N be positive integers. The number of lozenge tilings of a hexagon with sides N + 1, 2m - 1, N + 1, 2m - 1, N + 1, which

<sup>&</sup>lt;sup>28</sup>Doubly-symmetric would be more descriptive, but then naming the region obtained by translating the lozenge-shaped hole off the symmetry axis would become cumbersome.

<sup>&</sup>lt;sup>29</sup>Unlike in the current paper, in [17], the authors use a triangular lattice such that one family of lattice line is vertical. Thus, a horizontal symmetry axis in [17] corresponds to a vertical symmetry axis in the current paper.

<sup>&</sup>lt;sup>30</sup>The reason the formula is written as a prefactor times the shown triple product is that, by a classical result of MacMahon [27], the number of lozenge tilings of a hexagon of side-lengths a, b, c, a, b, c equals  $\prod_{i=1}^{a} \prod_{j=1}^{b} \prod_{k=1}^{c} \frac{i+j+k-1}{i+j+k-2}$ .

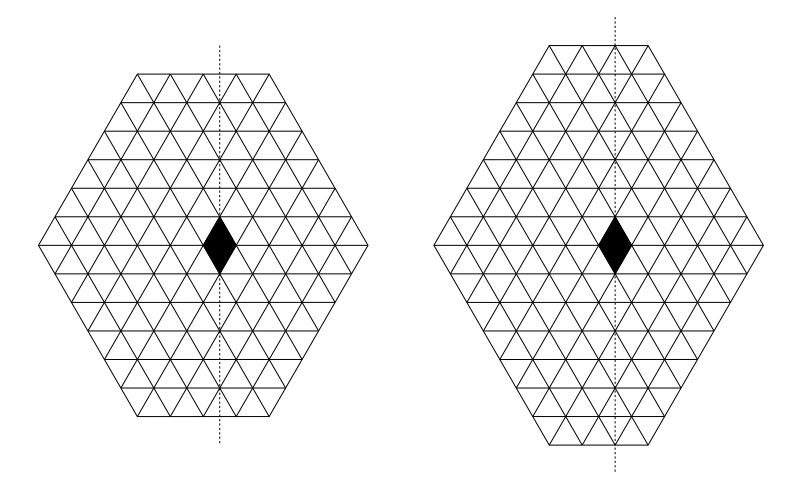


Figure 30: The regions considered in Theorem 19 (left) and Theorem 20 (right). These pictures illustrate the case when m=2 and n=3.

contain the l-th lozenge on the symmetry axis which cuts through the sides of length 2m-1, equals

$$\frac{m\binom{m+N}{m}\binom{m+N-1}{m}}{\binom{2m+2N-1}{2m}} \left( \sum_{e=0}^{l-1} (-1)^e \binom{N}{e} \frac{(N-2e)(\frac{1}{2})_e}{(m+e)(m+N-e)(\frac{1}{2}-N)_e} \right) \cdot \prod_{i=1}^{N+1} \prod_{j=1}^{N+1} \prod_{k=1}^{2m-1} \frac{i+j+k-1}{i+j+k-2}.$$
(67)

In [18] Fulmek and Krattenthaler considered the problem of enumerating lozenge tilings of a symmetric hexagon with a lozenge hole on the *horizontal* symmetry axis. Formulas were provided for three cases: when the lozenge hole is (1) a half unit, (2) one unit, and (3) one and a half units away from the vertical symmetry axis. We recall the two theorems in [18] that correspond to the first case (the two pictures in Figure 30 illustrate these regions).

**Theorem 19** (Theorem 1 in [18]). Let n and m be positive integers. The number of lozenge tilings of a hexagon with side lengths 2n, 2m, 2n, 2m, 2n (clockwise from top left), which contain the lozenge just to the right of the center of the hexagon, equals

$$\frac{nm\binom{2n}{n}\binom{2n-1}{n}\binom{2m}{m}}{\binom{4n+2m-1}{2n+m}} \left( -\frac{1}{(n+m)^2} + \frac{4n+2}{(n+1)(2n-1)(n+m-1)(n+m+1)} \right) \cdot \sum_{h=0}^{n-1} \frac{(2)_h(1-n)_h(\frac{3}{2}+n)_h(1-n-m)_h(1+n+m)_h}{(1)_h(2+n)_h(\frac{3}{2}-n)_h(2+n+m)_h(2-n-m)_h} \right) \cdot \prod_{i=1}^{2n} \prod_{j=1}^{2m} \prod_{k=1}^{2n} \frac{i+j+k-1}{i+j+k-2}.$$
(68)

**Theorem 20** (Theorem 2 in [18]). Let n be a non-negative integer and m a positive integer. The number of lozenge tilings of a hexagon with side lengths 2n + 1, 2m - 1, 2n + 1, 2m - 1, 2n + 1 (clockwise from top left), which contain the lozenge just to the right of the center of the hexagon, equals

$$\frac{(n+1)m\binom{2n}{n}\binom{2n+1}{n}\binom{2m-1}{m}}{\binom{4n+2m}{2n+m}} \left(\frac{1}{(n+m)^2} + \frac{4n}{(n+1)(2n-1)(n+m-1)(n+m+1)} \cdot \sum_{h=0}^{n-1} \frac{(2)_h(1-n)_h(\frac{3}{2}+n)_h(1-n-m)_h(1+n+m)_h}{(1)_h(2+n)_h(\frac{3}{2}-n)_h(2+n+m)_h(2-n-m)_h}\right) \cdot \prod_{i=1}^{2n+1} \prod_{j=1}^{2m-1} \prod_{k=1}^{2n+1} \frac{i+j+k-1}{i+j+k-2}.$$
(69)

Note that given a region R and a lozenge L inside the region, the lozenge tilings of R containing L can be identified with the lozenge tilings of the region obtained from R by creating a lozenge-shaped hole at location L. Thus, the four theorems above can be regarded as lozenge tiling enumerations of symmetric hexagons with unit lozenges removed.

The result we present in this section is an extension of Theorems 19 and 20 in the style of Theorems 17 and 18. For a non-negative integer m and a positive integer N, let V(N, 2m, l) be the region obtained from the symmetric hexagon of side-lengths 2m, N, N, 2m, N, N (clockwise from top) by deleting the l-th lozenge on the vertical symmetry axis. Similarly, let V'(N, 2m, l) be the region obtained from the same hexagon by deleting the l-th lozenge on the vertical axis that is half a unit to the right of the vertical symmetry axis.

Similarly, for positive integers m and N, let V(N+1,2m-1,l) be the region obtained from the symmetric hexagon of side-lengths 2m-1, N+1, N+1, 2m-1, N+1, N+1 (clockwise from top) by deleting the l-th lozenge on the vertical symmetry axis. Similarly, let V'(N+1,2m-1,l) be the region obtained from the same hexagon by deleting the l-th lozenge on the vertical axis that is half a unit to the right of the vertical symmetry axis.

The first two results of Fulmek and Krattenthaler stated above (Theorem 17 and 18) are about the number of lozenge tilings of the regions V(N, 2m, l) and V(N+1, 2m-1, l). The main results of this section (see Theorems 21 and 22 below) give formulas for the number of lozenge tilings of the regions V'(N, 2m, l) and V'(N+1, 2m-1, l), and thus extends the results of Fulmek and Krattenthaler quoted as Theorems 19 and 20 by lending them the generality of the context of their results quoted as Theorems 17 and 18.

**Theorem 21.** Let m be a positive integer and N be a positive integer greater than 1. The number of lozenge tilings of the region V'(N, 2m, l) obtained from the hexagon with sides

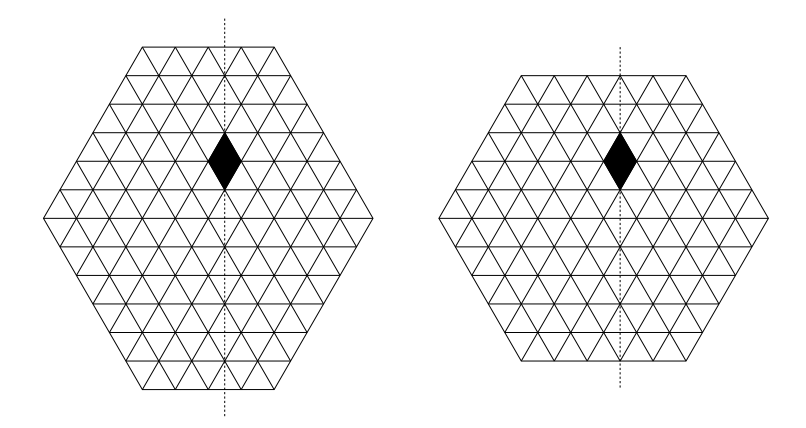


Figure 31: The regions considered in the current section. These two pictures illustrate V'(N, 2m, l) and V'(N - 1, 2m + 1, l) when m = 2, N = 6, and l = 2.

2m, N, N, 2m, N, N (clockwise from top) by deleting the l-th lozenge from the top on the vertical axis half a unit away from the vertical symmetry axis, is given by

$$M(V'(N,2m,l)) = \frac{(m+1)_N(m)_N(N)_{N-1}}{(2m+1)_N(2m+N)_N(N-1)!} \cdot \sigma_1(N,m,l) \cdot \prod_{i=1}^N \prod_{j=1}^N \prod_{k=1}^{2m} \frac{i+j+k-1}{i+j+k-2},$$
(70)

where

$$\sigma_{1}(N,m,l) = (2m+2N-1) \cdot \sum_{e=0}^{l-1} (-1)^{e} {N-1 \choose e} \frac{(N-2e-1)(\frac{1}{2})_{e}}{(m+e)(m+N-e-1)(\frac{3}{2}-N)_{e}} + (2m+1) \cdot \sum_{e=0}^{l-1} (-1)^{e} {N-1 \choose e} \frac{(N-2e-1)(\frac{1}{2})_{e}}{(m+e+1)(m+N-e)(\frac{3}{2}-N)_{e}}.$$

$$(71)$$

**Theorem 22.** Let m be a non-negative integer and N be a positive integer greater than 1. The number of lozenge tilings of the region V'(N-1,2m+1,l) obtained from the hexagon of sides 2m+1, N-1, N-1, 2m+1, N-1, N-1 (clockwise from top) by deleting the l-th lozenge from the top on the vertical axis half a unit away from the vertical symmetry axis, is given by

$$M(V'(N-1,2m+1,l)) = \frac{(m+1)_{N-1}(m+1)_{N-1}(N-1)_{N-1}}{(2m+2)_{N-1}(2m+N)_{N-1}(N-1)!} \cdot \sigma_2(N,m,l) \cdot \prod_{i=1}^{N-1} \prod_{j=1}^{N-1} \prod_{k=1}^{2m+1} \frac{i+j+k-1}{i+j+k-2},$$
(72)

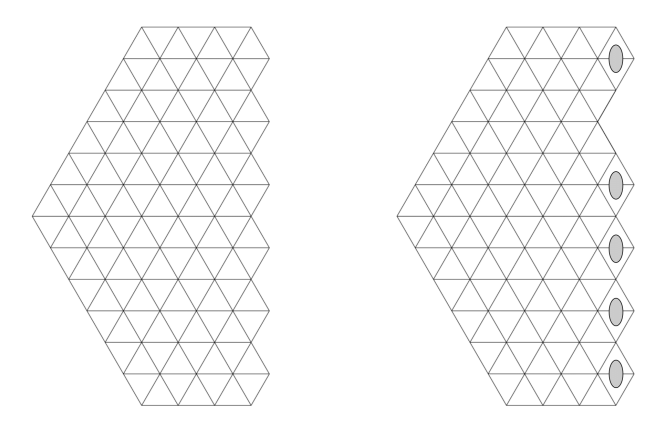


Figure 32: Left. The region S(N, m) for N = 6 and m = 3. Right. The region C(N, m, l) for N = 6, m = 3 and l = 2. Lozenges marked by ellipses are weighted by  $\frac{1}{2}$ , as in the previous sections.

where

$$\sigma_{2}(N,m,l) = m \cdot \sum_{e=0}^{l-1} (-1)^{e} {N-1 \choose e} \frac{(N-2e-1)(\frac{1}{2})_{e}}{(m+e)(m+N-e-1)(\frac{3}{2}-N)_{e}} + (m+N) \cdot \sum_{e=0}^{l-1} (-1)^{e} {N-1 \choose e} \frac{(N-2e-1)(\frac{1}{2})_{e}}{(m+e+1)(m+N-e)(\frac{3}{2}-N)_{e}}.$$

$$(73)$$

We deduce the above two results from Theorem 2, using also enumeration results on certain families of regions given in [17]. Although one of them is a special case of a region we considered in an earlier section, for consistency with [17] we use the notation from there.

For non-negative integers m and N, let S(N,m) be the pentagonal region depicted on the left in Figure 32; note that this region was previously denoted by  $\overline{R}_{(1,\ldots,N),\emptyset}(m)$  in subsection 4.2. Also, for a non-negative integer m and positive integers l and N such that  $l \leq N$ , we define the region C(N,m,l) as follows: on S(N,m), we label the N rightmost vertical lozenges by  $1,\ldots,N$ , from top to bottom. Then we remove the vertical lozenge labeled by l and assign the weight  $\frac{1}{2}$  to the remaining N-1 vertical lozenges (see the picture on the right in Figure 32). In [17], Fulmek and Krattenthaler determined the number of lozenge tilings for S(N,m) and the weighted count of lozenge tilings<sup>31</sup> of C(N,m,l).

**Lemma 23.** ((2.4) and (2.6) in [17]) For any non-negative integer m and positive integer N,

$$M(S(N,m)) = \prod_{i=1}^{N} \frac{(N+m-i+1)!(i-1)!(2m+i+1)_{i-1}}{(m+i-1)!(2N-2i+1)!}.$$
 (74)

<sup>&</sup>lt;sup>31</sup>Our formula looks somewhat different compared to the one provided in [17] since we made some simplifications in the latter.

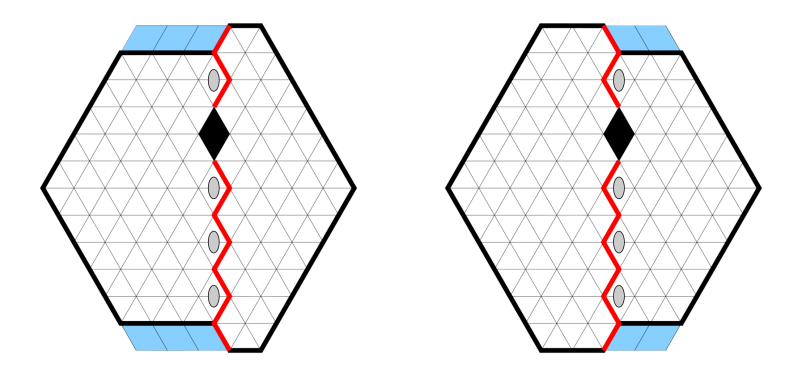


Figure 33: One of the two zigzag lines splits V'(4,6,2) into the subregions C(5,3,2) and S(6,1) (left). The other zigzag line splits it into C(5,2,2) and S(6,2) (right).

**Lemma 24.** ((2.5) and (2.7) in [17]) For any non-negative integer m and positive integers l and N such that  $l \leq N$ ,

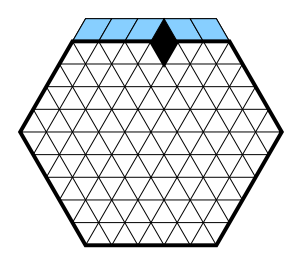
$$M(C(N, m, l)) = \frac{(m)_{N+1}}{2^{N-1}N!} \prod_{i=1}^{\lfloor \frac{N}{2} \rfloor} \frac{(2m+2i)_{2N-4i+1}}{(2i)_{2N-4i+1}} \cdot \sum_{e=0}^{l-1} (-1)^e {N \choose e} \frac{(N-2e)(\frac{1}{2})_e}{(m+e)(m+N-e)(\frac{1}{2}-N)_e}.$$
(75)

Proof of Theorem 21. We apply Theorem 2 to the region V'(N, 2m, l). To do that, we split the region using the two different zigzag lines along the vertical axis through the hole. While one of the zigzag lines splits the region into S(N, m) and C(N-1, m, l), the other splits it into S(N, m-1) and C(N-1, m+1, l) (see the two pictures in Figure 33). Thus, by Theorem 2, we have

$$M(V'(N, 2m, l)) = 2^{N-2} \Big[ M(S(N, m)) M(C(N-1, m, l)) + M(S(N, m-1)) M(C(N-1, m+1, l)) \Big].$$
(76)

By combining (74), (75), (76) and factoring out some common factors, we get the desired formula for M(V'(N, 2m, l)).

Proof of Theorem 22. Theorem 2 is not applicable when l=1, because the region  $R_0$  is not well-defined. Because of this, we consider the case l=1 separately. In this case, the region V'(N-1,2m+1,1) can be regarded as a trapezoid region with dents on its base (see Figure 34 and the explanation in its caption). The number of lozenge tilings of such regions was given in [11, Proposition 2.1] and one can check that the l=1 specialization of our claimed formula agrees with the expression obtained using [11, Proposition 2.1]. Assume therefore that  $l \geq 2$ , and apply Theorem 2. To do that, we again consider



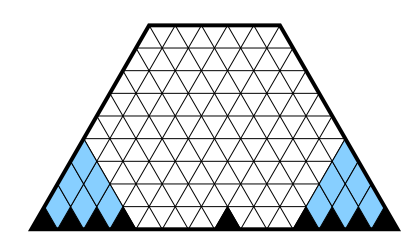
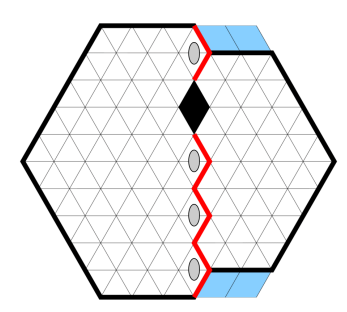


Figure 34: If we remove the forced lozenges from the region V'(N, m, 1) on the left (here N = 5 and m = 5), and also from the region on the right (which is a special case of the regions whose tilings are enumerated by Proposition 2.1 of [11]), the two resulting regions are congruent.



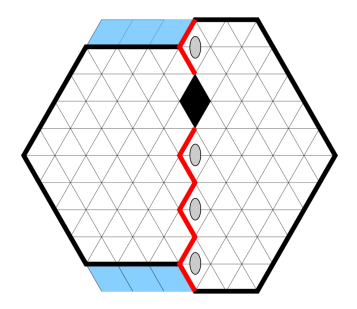


Figure 35: One of the two zigzag lines splits V'(5,5,2) into the subregions C(5,3,2) and S(4,2) (left). The other splits it into C(5,2,2) and S(4,3) (right).

the two zigzag lines along the vertical symmetry axis of the lozenge hole. One of them divides the region into S(N-2,m) and C(N-1,m+1,l), while the other divides it into S(N-2,m+1) and C(N-1,m,l) (see Figure 35. Thus, by Theorem 2, we obtain

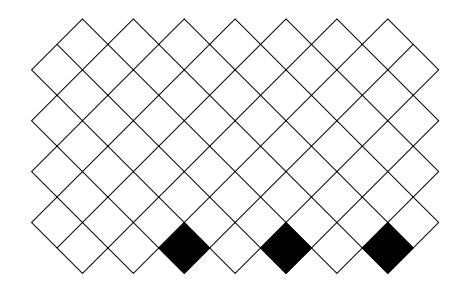
$$M(V'(N-1,2m+1,l)) = 2^{N-3} \Big[ M(S(N-2,m)) M(C(N-1,m+1,l)) + M(S(N-2,m+1)) M(C(N-1,m,l)) \Big].$$
(77)

Using (74), (75), (77) and factoring out some common factors, we get the claimed formula for M(V'(N+1,2m-1,l)).

## 7 Aztec rectangles with collinear unit holes

Let m and n be positive integers with  $m \leq n$ . The  $m \times n$  Aztec rectangle, denoted by AR(m,n), is the region consisting of all unit squares on  $\mathbb{Z}^2$  whose centers (x,y) satisfy the inequalities  $|x| + |y| \leq n$  and  $x + y \geq n - 2m$ . In this section, we rotate the region AR(m,n) by 45° in counterclockwise direction (see the pictures in Figure 36; at this point, ignore the black unit squares in the pictures).

Unless m = n (when it becomes the Aztec diamond  $AD_n$ ), the Aztec rectangle AR(m, n) does not have any domino tilings: it is not hard to check that if we color the square grid



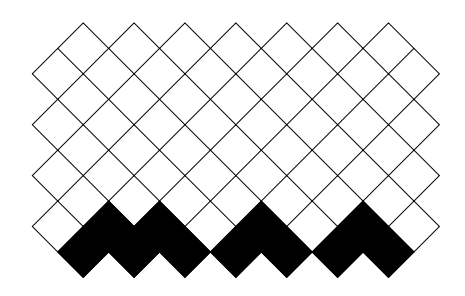


Figure 36: The regions  $AR(4,7;\{1,2,4,6\})$  (left) and  $\overline{AR}(4,7;\{2,3,5,7\})$  (right). Both regions are obtained from AR(4,7) by deleting some unit squares.

in chessboard fashion, AR(m,n) has n-m more unit squares of one color than the other. This can be fixed as follows. Label the bottom-most unit squares in AR(m,n) by  $1, \ldots, n$  from left to right. For any subset  $S \subseteq [n] := \{1, \ldots, n\}$  of size m, we delete the unit squares labeled with elements of  $[n] \setminus S$  from AR(m,n), and denote the resulting region by AR(m,n;S) (see the picture on the left in Figure 36 for an illustration). Then the region AR(m,n;S) always admits domino tilings; the number of them is given by (see [4] [16] [28])

$$M(AR(m, n; S)) = 2^{m(m+1)/2} \prod_{1 \le i < j \le m} \frac{s_j - s_i}{j - i},$$
(78)

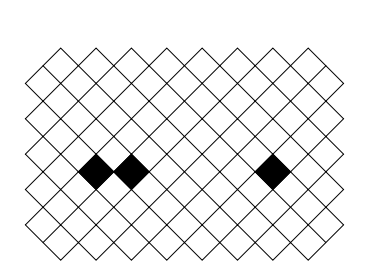
where  $S = \{s_1, ..., s_m\}$ , with  $s_1 < \cdots < s_m$ .

Next, for any subset  $T = \{t_1, \ldots, t_m\} \subseteq \{n+1\}$  of size m (again, with elements of T written in increasing order), consider the region  $\overline{AR}(m,n;T)$  defined as follows. From AR(m,n), remove the n unit squares at the bottom. Note that the resulting region has n+1 unit squares on the (new) bottom. Label these unit squares by  $1,\ldots,n+1$ , from left to right. Finally, delete the unit squares labeled by elements of T, and denote the resulting region by  $\overline{AR}(m,n;T)$ . The number of domino tilings for this region was studied in [16] and [19], and is given by

$$M(\overline{AR}(m, n; T)) = 2^{m(m-1)/2} \prod_{1 \le i < j \le m} \frac{t_j - t_i}{j - i},$$
 (79)

In [4], the second author proved that if an arbitrary collection of unit squares is deleted from the horizontal symmetry axis of an Aztec rectangle, the number of domino tilings of the resulting region is given by a simple product formula. More precisely, let m and N be positive integers with  $2m \leq N$ . Then the number of domino tilings of a  $2m \times N$  Aztec rectangle, where all the unit squares on the central horizontal row, except the  $t_1$ -st, the  $t_2$ -nd,..., and the  $t_2m$ -th unit square have been removed equals

$$\frac{2^{m^2+2m}}{\prod_{i=1}^{m} (i-1)!^2} \prod_{1 \le i < j \le m} (t_{2j} - t_{2i}) \prod_{1 \le i < j \le m} (t_{2j-1} - t_{2i-1}). \tag{80}$$



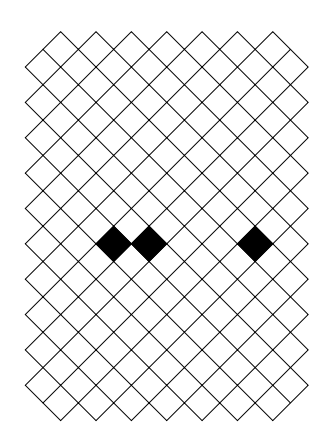


Figure 37: A picture that illustrates Theorem 25 with m=2, N=8, and  $(t_1,t_2,t_3,t_4,t_5)=(1,4,5,6,8)$  (left) and another picture that illustrates Theorem 26 with m=5, N=7, and  $(t_1,t_2,t_3,t_4,t_5)=(1,2,5,6,8)$  (left). Later when we prove Theorem 27, the picture on the left is denoted by  $R_1(2m+1,N;(t_1,\ldots,t_{2m+1}))=R_1(5,8;(1,4,5,6,8))$ .

This was extended by Krattenthaler [21], who considered the following more general question: if we delete collinear unit squares along an *arbitrary* horizontal line from an Aztec rectangle, what is the number of domino tilings of the resulting regions<sup>32</sup>? Using certain Schur function identities, he answered this question by finding some explicit formulas.

As equation (80) shows, the special case when the horizontal axis containing the deleted unit squares is the symmetry axis, this formula becomes a simple product formula. Furthermore, the special case of Krattenthaler's formula when the line containing the deleted squares is just below the symmetry axis also turns out to be a simple product formula.

**Theorem 25** (Theorem 9 in [21]). Let m and N be positive integers with  $2m + 1 \leq N$ . Then the number of domino tilings of a  $(2m + 1) \times N$  Aztec rectangle, where all the unit squares on the horizontal row that is just below the central row, except for the  $t_1$ -st, the  $t_2$ -nd,..., and the  $t_{2m+1}$ -th unit square, have been removed (see the left picture in Figure 37), equals

$$\frac{2^{m^2+3m+1}}{\prod\limits_{i=1}^{m}(i-1)!\prod\limits_{i=1}^{m+1}(i-1)!}\prod\limits_{1\leqslant i< j\leqslant m}(t_{2j}-t_{2i})\prod\limits_{1\leqslant i< j\leqslant m+1}(t_{2j-1}-t_{2i-1}).$$
(81)

**Theorem 26** (Theorem 10 in [21]). Let m and N be positive integers with  $2m \ge N$ . Then the number of domino tilings of a  $2m \times N$  Aztec rectangle, where all the unit squares on the horizontal row that is just below the central row, except for the  $t_1$ -st, the  $t_2$ -nd,..., and

<sup>&</sup>lt;sup>32</sup>In fact, Krattenthaler expressed this in terms of perfect matchings of the planar dual graphs. In this paper, in order to be consistent with the previous sections, we state everything in terms of domino tilings.

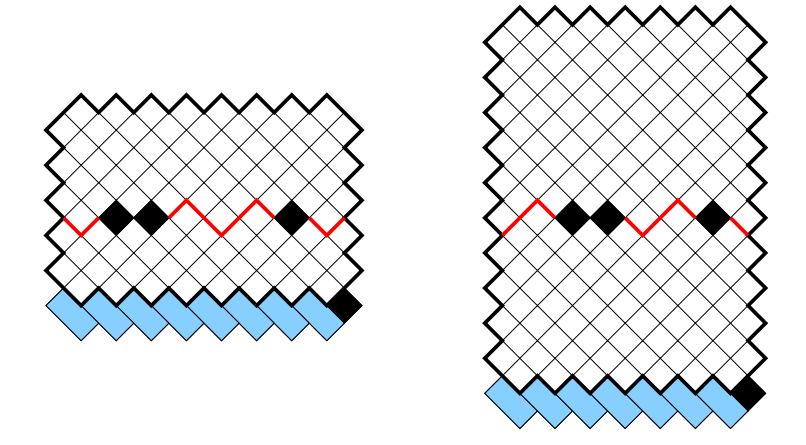


Figure 38: Application of Theorem 1(b) to the two regions in Figure 37.

the  $t_{2N-2m+1}$ -th unit square, have been removed (see the right picture in Figure 37), equals

$$2^{m^{2}-m+N} \frac{\prod_{i=m+1}^{N+1} (i-1)! \prod_{i=m+2}^{N+1} (i-1)!}{\prod_{i=1}^{N+1} (t_{i}-1)! (N+1-t_{i})!} \times \prod_{1 \leq i < j \leq N-m} (t_{2j}-t_{2i}) \prod_{1 \leq i < j \leq N-m+1} (t_{2j-1}-t_{2i-1}).$$
(82)

Krattenthaler's proofs of Theorems 25–26 in [21] were based on certain Schur function identities. In this section, we give a very simple proof of these theorems using Theorem 1.

Proof of Theorems 25–26. We first prove Theorem 25. To do that, we add one layer at the bottom of the region by adding 2N+1 unit squares that form a zigzag path, and then we delete the rightmost newly added unit square (see the left picture in Figure 38). Then, the dual graph of the resulting region is a symmetric graph with a vertex removed from its boundary, to which Theorem 1(b) can be applied. If we apply Theorem 1(b) to this dual graph, take the dual again, and delete the forced dominos, we get that the number of domino tilings of the region in Theorem 25 can be expressed as follows:

$$2^{m} M(AR(m+1, N; \{t_{2i-1}\}_{i \in [m+1]})) M(AR(m, N; \{t_{2i}\}_{i \in [m]})).$$
(83)

Combining (78) and (83) one obtains (81), which completes the proof of Theorem 25.

The same approach works for proving Theorem 26. We add one layer at the bottom of the Aztec rectangle by including 2N + 1 unit squares in the same way as in the proof of Theorem 25, and then remove the rightmost of these (see the picture on the right in Figure 38). We can again apply Theorem 1(b), and after removing the forced forced dominos of the resulting regions, we obtain that the number sought in Theorem 26 equals

$$2^{N-m} M(\overline{AR}(m, N; [N+1] \setminus \{t_{2i-1}\}_{i \in [N-m+1]})) M(\overline{AR}(m+1, N; [N+1] \setminus \{t_{2i}\}_{i \in [N-m]})).$$
(84)

Combining (79) and (84) one gets (82), which proves Theorem 26.

We finish this section by presenting one more new proof, namely of the following theorem, which is another special case of Krattenthaler's general result (Theorem 11 in [21]).

**Theorem 27** (The case d = 2 in Theorem 11 in [21]). Let m and N be positive integers with  $2m + 2 \le N$ . Then the number of domino tilings of a  $(2m + 2) \times N$  Aztec rectangle, where all the unit squares on the horizontal row that is by 2 below the central row, except for the  $t_1$ -st, the  $t_2$ -nd,..., and the  $t_{2m+2}$ -th unit square, have been removed, equals

$$\frac{2^{m^2+4m+3}}{\prod_{i=1}^{m}(i-1)!} \cdot \left[ \prod_{1 \le i < j \le m+1} (t_{2j} - t_{2i})(t_{2j-1} - t_{2i-1}) \right] \cdot \left( \sum_{i=1}^{2m+2} (-1)^i t_i \right). \tag{85}$$

Note that our formula (85) has a simpler form than Krattenthaler's original formula (see (4.5) in [21]; it is not so straightforward to show that the second line in the d=2 specialization of that formula equals  $\sum_{i=1}^{2m+2} (-1)^i t_i$ ). Krattenthaler's proof of the above theorem used some Schur function identities. By contrast, we prove this theorem using Kuo's graphical condensation method. Although we stated Kuo's condensation theorem in Section 2 (see Theorem 3), we state here a different version of it, because this is the one we need in our proof of Theorem 27.

**Theorem 28** (Theorem 2.1 in [22]). Let  $G = (V_1, V_2, E)$  be a plane bipartite graph in which  $|V_1| = |V_2|$ . Let vertices a, b, c, and d appear in a cyclic order on the same face of G. If  $a, c \in V_1$  and  $b, d \in V_2$ , then

$$M(G) M(G \setminus \{a, b, c, d\}) = M(G \setminus \{a, c\}) M(G \setminus \{b, d\}) + M(G \setminus \{a, d\}) M(G \setminus \{b, c\}).$$

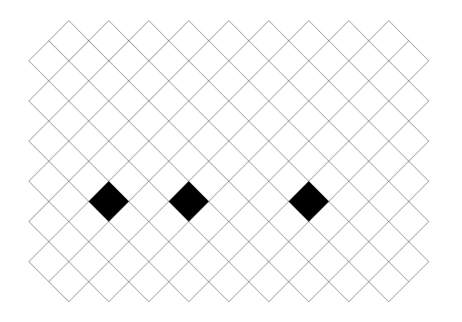
Let

- $R_0(2m, N; \{t_1, \ldots, t_{2m}\})$  be the region described just before equation (80),
- $R_1(2m+1, N; \{t_1, \ldots, t_{2m+1}\})$  be the region described in Theorem 25, and
- $R_2(2m+2, N; \{t_1, \ldots, t_{2m+2}\})$  be the region described in Theorem 27.

Under this notation, we want to show that the number of domino tilings of  $R_2(2m + 2, N; \{t_1, \ldots, t_{2m+2}\})$  is given by (85). Note that the region  $R_2(2m+2, N; \{t_1, \ldots, t_{2m+2}\})$  has N - (2m+2) unit square holes in it. This is important because we will use an induction on this quantity.

Proof of Theorem 27. Note that it suffices to prove the statement of Theorem 27 for the regions  $R_2(2m+2, N; \{t_1, \ldots, t_{2m+2}\})$  with  $t_1 = 1$  and  $t_{2m+2} = N$ . Indeed, if  $t_1 \neq 1$  or  $t_{2m+2} \neq N$ , then by deleting some forced dominos, one obtains a smaller region with fewer holes in it.

We first construct a recurrence relation using Kuo's graphical condensation (Theorem 28). Consider a region  $R_2(2m+2, N; \{t_1, \ldots, t_{2m+2}\})$  with  $t_1 = 1$  and  $t_{2m+2} = N$ . Add



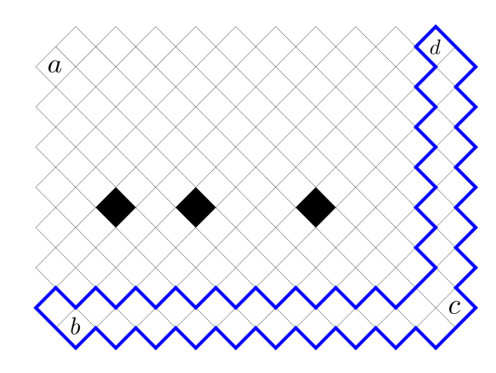


Figure 39:  $R_2(2m+2, N, \{t_1, \ldots, t_{2m+2}\}) = R_2(6, 9; \{1, 3, 5, 6, 8, 9\})$  (left) and  $R_1(2m+3, N+1; \{t_1, \ldots, t_{2m+2}, N+1\}) = R_1(7, 10, \{1, 3, 5, 6, 8, 9, 10\})$  (right). The region on the right is obtained from the one on the left by adding a layer along the bottom and right sides. The extended part is marked by thick blue lines; four unit squares a, b, c, and d are also marked.

a layer on the bottom and right sides of this region, as described in Figure 39. On this extended region, we choose four unit squares a, b, c, and d as shown in the picture on the right in Figure 39. The dual graph of the extended region, together with its four vertices corresponding to the unit squares labeled by a, b, c, and d, satisfies the conditions required in Theorem 28. If we apply Kuo's graphical condensation on this dual graph, take the dual again, and remove the forced dominos in the resulting regions, we obtain the following recurrence relation (see the six regions in Figure 40):

$$M(R_{1}(2m+3, N+1; \{t_{1}, ..., t_{2m+2}, N+1\})) \cdot M(R_{1}(2m+1, N-1; \{t_{2}-1, ..., t_{2m+2}-1\})) = M(R_{2}(2m+2, N; \{t_{2}-1, ..., t_{2m+2}-1, N\})) M(R_{0}(2m+2, N; \{t_{1}, ..., t_{2m+2}\})) + M(R_{2}(2m+2, N; \{t_{1}, ..., t_{2m+2}\})) M(R_{0}(2m+2, N; \{t_{2}-1, ..., t_{2m+2}-1, N\})).$$
(86)

One can check that the expressions on the right hand sides of equations (80), (81) and (85) satisfy the above recurrence relation (86). Using this, we will give an inductive proof of Theorem 27. We start the proof with an induction on the number of holes in the region  $R_2(2m+2, N; \{t_1, \ldots, t_{2m+2}\})$ , which is N-(2m+2). Let us call this the *outer induction*.

When N-(2m+2)=0,  $\{t_1,\ldots,t_{2m+2}\}=[2m+2]$  (where  $[n]:=\{1,2,\ldots,n\}$ ) and the region  $R_2(2m+2,N;\{t_1,\ldots,t_{2m+2}\})=R_2(2m+2,2m+2;[2m+2])$  becomes the Aztec diamond of order 2m+2. One can check that if we set N=2m+2 and  $\{t_1,\ldots,t_{2m+2}\}=[2m+2]$  in the expression on the right hand side of (85), we get  $2^{\frac{(2m+2)(2m+3)}{2}}$ , which is the number of domino tilings of the Aztec diamond of order 2m+2. Thus, the theorem is verified for the case when N-(2m+2)=0.

Suppose Theorem 27 holds whenever N-(2m+2) < k for some positive integer k. Under this assumption, we need to show that the theorem still holds when N-(2m+2)=k. To show this, we need another induction. This time we induct on the smallest element of

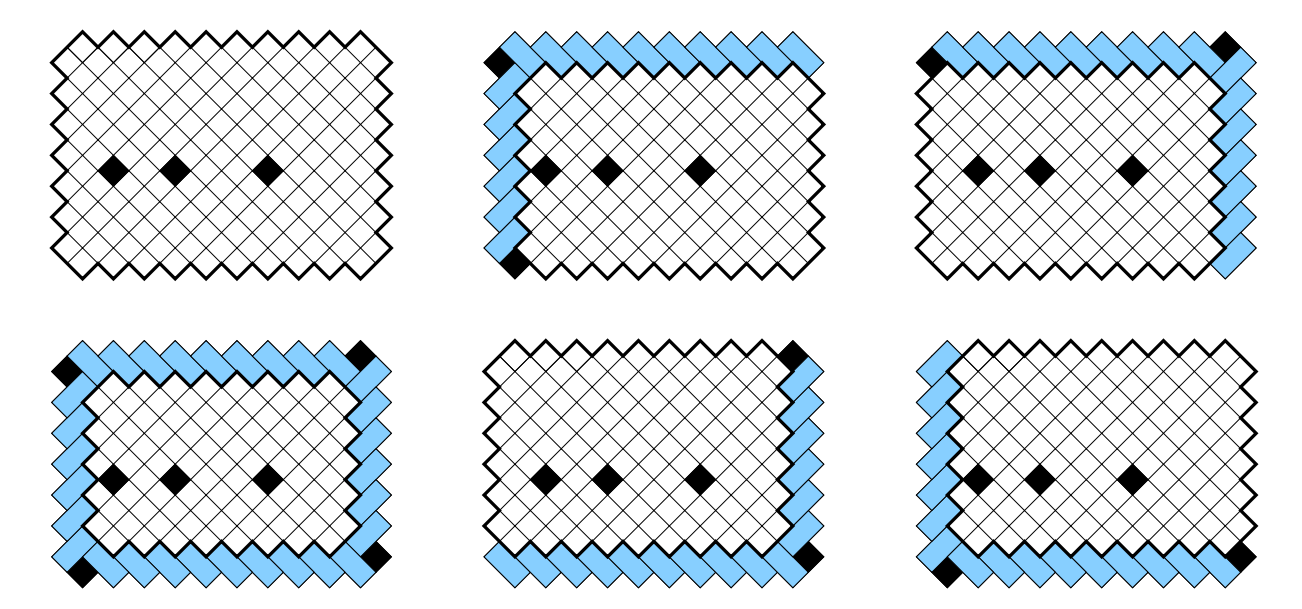


Figure 40: The six regions appearing in the recurrence relation we obtain by applying Kuo's graphical condensation to the region in the picture on the right in Figure 39.

 $[N] \setminus \{t_1, \ldots, t_{2m+2}\}$ . We call this the *inner induction*. If the smallest element is 1, then the unit square labeled 1 was removed. But this causes several forced dominos on the left side of the region. Due to this, in this case, the region  $R_2(2m+2, N; \{t_1, \ldots, t_{2m+2}\})$  can be identified with  $R_2(2m+2, N-1; \{t_1-1, \ldots, t_{2m+2}-1\})$ , which is the region whose number of domino tilings is given by (85) by the outer induction hypothesis. Thus we have checked the case when the smallest element of  $[N] \setminus \{t_1, \ldots, t_{2m+2}\}$  is 1.

Now suppose that Theorem 27 holds when N-(2m+2)=k and the smallest element of  $[N]\setminus\{t_1,\ldots,t_{2m+2}\}$  is less than or equal to a positive integer l. Under this assumption, we need to show that the theorem still holds when N-(2m+2)=k and the smallest element of  $[N]\setminus\{t_1,\ldots,t_{2m+2}\}$  is l+1. Consider the recurrence relation (86), and focus on the two terms containing an  $R_2$ -region. It is not difficult to check that when  $t_1=1$  (which is the case, as we can now assume that the smallest element of  $[N]\setminus\{t_1,\ldots,t_{2m+2}\}$  is j=1, the smallest element of j=1 is greater than that of j=1 is j=1, the smallest element of j=1 is greater than that of j=1 is j=1 in and it exceeds the latter by exactly one. Since we already checked that (86) is satisfied by (80), (81), and (85), we can conclude that Theorem 27 also holds when j=1 is j=1. Thus, the inner induction is checked, and it follows that Theorem 27 always holds whenever j=1 in j=1 induction step is verified for the outer induction, and it follows that Theorem 27 holds whenever j=1 is j=1 in an on-negative integer. This completes the proof.

## Acknowledgements

Part of this research was performed while the first author was visiting the Institute for Pure and Applied Mathematics (IPAM), which is supported by the National Science Foundation (Grant No. DMS-1925919). He would like to thank the program organizers

and IPAM staff members for their hospitality during his stay in Los Angeles. The first author thanks the American Mathematical Society and Simons foundations for supporting in part his work by AMS-Simons Travel Grant. The second author thanks the Simons Foundation for supporting in part his work by Simons Foundation Collaboration Grant 710477. The authors would also like to thank the referee for the careful reading of the manuscript and for helpful suggestions.

## References

- [1] S. H. Byun. Lozenge tilings of a hexagon with a horizontal intrusion. *Ann. Comb.*, 26(4):943–970, 2022.
- [2] S. H. Byun and M. Ciucu. Perfect matchings and spanning trees: squarishness, bijections and independence. arXiv:2404.09930, 2024.
- [3] S. H. Byun and T. Lai. Lozenge tilings of hexagons with intrusions I: Generalized intrusion. Adv. in Appl. Math., 162, Paper No. 102775, 2025.
- [4] M. Ciucu. Enumeration of perfect matchings in graphs with reflective symmetry. *J. Combin. Theory Ser. A*, 77(1):67–97, 1997.
- [5] M. Ciucu. A random tiling model for two dimensional electrostatics. *Mem. Amer. Math. Soc.*, 178(839):x+144, 2005.
- [6] M. Ciucu. The other dual of MacMahon's theorem on plane partitions. *Adv. Math.*, 306:427–450, 2017.
- [7] M. Ciucu. Symmetries of shamrocks II: Axial shamrocks. *Electron. J. Combin.*, #P2.36, 2018.
- [8] M. Ciucu and C. Krattenthaler. Plane partitions II:  $5\frac{1}{2}$  symmetry classes. In *Combinatorial methods in representation theory*, volume 28 of *Adv. Stud. Pure Math.*, pages 81–101. Mathematical Society of Japan, 2000.
- [9] M. Ciucu and C. Krattenthaler. A dual of MacMahon's theorem on plane partitions. *Proc. Natl. Acad. Sci. USA*, 110(12):4518–4523, 2013.
- [10] M. Ciucu, T. Lai, and R. Rohatgi. Tilings of hexagons with a removed triad of bowties. *J. Combin. Theory Ser. A*, 178:105359, 2021.
- [11] H. Cohn, M. Larsen, and J. Propp. The shape of a typical boxed plane partition. New York J. Math., 4(137):165, 1998.
- [12] S. Corteel, F. Huang, and C. Krattenthaler. Domino tilings of generalized aztec triangles. arXiv:2305.01774, 2023.
- [13] C. Defant, L. Foster, R. Li, J. Propp, and B. Young. Tilings of benzels via generalized compression. SIAM J. Discrete Math., 39, 146-162.
- [14] C. Defant, R. Li, J. Propp, and B. Young. Tilings of benzels via the abacus bijection. Comb. Theory, 3(2), 2023.
- [15] P. Di Francesco. Twenty vertex model and domino tilings of the Aztec triangle. *Electron. J. Combin.*, #P4.38, 2021.

- [16] N. Elkies, G. Kuperberg, M. Larsen, and J. Propp. Alternating-sign matrices and domino tilings (part I,II). *J. Algebraic Combin.*, 1:111–132, 219–234, 1992.
- [17] M. Fulmek and C. Krattenthaler. The number of rhombus tilings of a symmetric hexagon which contain a fixed rhombus on the symmetry axis, I. *Ann. Comb.*, 2:19–41, 1998.
- [18] M. Fulmek and C. Krattenthaler. The number of rhombus tilings of a symmetric hexagon which contain a fixed rhombus on the symmetry axis, II. *European J. Combin.*, 21(5):601–640, 2000.
- [19] I. Gessel and H. Helfgott. Enumeration of tilings of diamonds and hexagons with defects. *Electron. J. Combin.*, 6:#R16, 1999.
- [20] J. Kim and J. Propp. A pentagonal number theorem for tribone tilings. *Electron. J. Combin.*, pages #P3.26, 2023.
- [21] C. Krattenthaler. Schur function identities and the number of perfect matchings of holey aztec rectangles. In q-Series from a Contemporary Perspective: AMS-IMS-SIAM Joint Summer Research Conference on Q-Series, Combinatorics, and Computer Algebra, June 21-25, 1998, Mount Holyoke College, South Hadley, MA, volume 254 of Contemp. Math., pages 335–349. American Mathematical Soc., 2000.
- [22] E. H. Kuo. Applications of graphical condensation for enumerating matchings and tilings. *Theoret. Comput. Sci.*, 319(1-3):29–57, 2004.
- [23] T. Lai. Lozenge tilings of a halved hexagon with an array of triangles removed from the boundary, Part II. *Electron. J. Combin.*, #P4.58, 2018.
- [24] T. Lai. Problems in the enumeration of tilings. In *Open problems in algebraic combinatorics*, volume 110 of *Proc. Sympos. Pure Math.*, pages 293–332. Amer. Math. Soc., Providence, RI, [2024] ©2024.
- [25] T. Lai and R. Rohatgi. Enumeration of lozenge tilings of a hexagon with a shamrock missing on the symmetry axis. *Discrete Math.*, 342(2):451–472, 2019.
- [26] T. Lai and R. Rohatgi. A shuffling theorem for lozenge tilings of doubly-dented hexagons. arXiv:1905.08311, 2019.
- [27] P. A. MacMahon. *Combinatory analysis*, volume I and II. Cambridge University Press, 1915-1916. repreinted in one volume by Chelsea, New York, 1960.
- [28] W. H. Mills, D. P. Robbins, and H. Rumsey Jr. Alternating sign matrices and descending plane partitions. *J. Combin. Theory Ser. A*, 34(3):340–359, 1983.
- [29] L. Pachter Combinatorial approaches and conjectures for 2-divisibility problems concerning domino tilings of polyominoes *Electron. J. Combin.*, 4:#R29, 1997.
- [30] J. Propp. Trimer covers in the triangular grid: twenty mostly open problems. In Open problems in algebraic combinatorics, volume 110 of Proc. Sympos. Pure Math., pages 261–273. Amer. Math. Soc., Providence, RI, [2024] ©2024.